R-1609

AD 747349
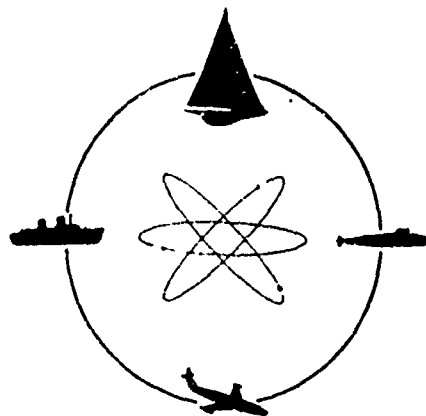
DAVIDSON
LABORATORY

Report SIT-DL-72-1609

June 1972

INVESTIGATION OF THE CORNERING DYNAMICS
OF A MILITARY TIRE

by
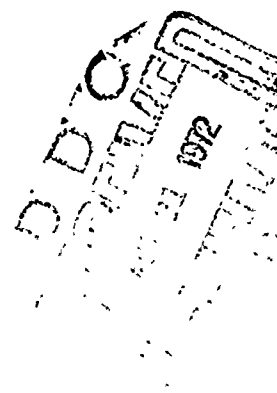
John E. Longhouser

STEVENS INSTITUTE
OF TECHNOLOGY

CASTLE POINT STATION
HOBOKEN, NEW JERSEY 07030

NATIONAL TECHNICAL
INFORMATION SERVICE

R-1609

DOCUMENT CONTROL DATA · R & D

(Security classification of title, body of abstract and indexing annotation must be entered when the overall report is classified)

1. ORIGINATING ACTIVITY (Corporate author)	2a. REPORT SECURITY CLASSIFICATION
Davidson Laboratory, Stevens Institute of Technology Hoboken, New Jersey 07030	UNCLASSIFIED
	2b. GROUP

3. REPORT TITLE

INVESTIGATION OF THE CORNERING DYNAMICS OF A MILITARY TIRE

4. DESCRIPTIVE NOTES (Type of report and inclusive dates)

Final Report

5. AUTHOR(S) (First name, middle initial, last name)

John Edward Longhouser

6. REPORT DATE	7a. TOTAL NO. OF PAGES	7b. NO. OF REFS
June 1972	66	10

8a. CONTRACT OR GRANT NO.	9a. ORIGINATOR'S REPORT NUMBER(S)
DAAE-07-69-0356	
b. PROJECT NO.	R-1609
c.	9b. OTHER REPORT NO(S) (Any other numbers that may be assigned this report)
d.	

10. DISTRIBUTION STATEMENT This document has been approved for public release and sale; its distribution is unlimited. ~~Application for copies may be made to the Defense Documentation Center, Cameron Station, 5010 Duke St., Alexandria, Va., 00314.~~ Reproduction of the document in whole or in part is permitted for any purpose of the U.S. Government

11. SUPPLEMENTARY NOTES	12. SPONSORING MILITARY ACTIVITY
	Department of Defense Washington, D. C. 20301

13. ABSTRACT

A review of a particular theoretical tire dynamics model is presented leading to a prediction of side thrust as the result of combined slip angle and camber angle with load as the major parameter. An experimental program to test these predictions was accomplished using 7.00-16 NDCC military tires mounted on a solid axle, unsprung toe-in trailer. The theoretical predictions did not compare well with the experimental results.

i

14. KEY WORDS	LINK A		LINK B		LINK C	
	ROLE	WT	ROLE	WT	ROLE	WT
Camber						
Camber Stiffness						
Cornering Stiffness						
Vehicle Dynamics						
Tires						

STEVENS INSTITUTE OF TECHNOLOGY
DAVIDSON LABORATORY
CASTLE POINT STATION
HOBOKEN, NEW JERSEY

Report SIT-DL-72-1609

June 1972

INVESTIGATION OF THE CORNERING DYNAMICS
OF A MILITARY TIRE

by

John Edward Longhouser

Prepared for

Department of Defense

under

Contract DAAE-07-69-0356

(DL Project 3683/423)

Approved

I. Robert Ehrlich, Manager
Transportation Research Group

TABLE OF CONTENTS

LIST OF SYMBOLS

A_0, A_1, A_2, A_3, A_4	Constant coefficients in parabolas fitted to tire side force properties
C_{co}	Small angle camber stiffness
C_{so}	Small angle cornering stiffness
D	The drag component of the tire side force (opposite to the wheel center velocity vector)
F_c	Tire cornering force, the lateral component of the tire side force (perpendicular to wheel center velocity vector)
F_n	Tire force perpendicular to the tire-terrain contact plane
F_o	Tire force component of $\overline{F}_s + F_n$ in tire center plane
F_s	Tire side force, the force in the plane of the tire-terrain contact patch, perpendicular to the line of intersection of the wheel plane and ground planes
F_s'	Tire side force resulting from the sum of the slip angle and the "equivalent" slip angles that approximate camber effects
F_{sc}	Side force due to camber angle
F_{ss}	Side force due to slip angle
$\vec{u}$	Velocity vector of the tire center parallel to the x-axis
$\vec{u}'$	Velocity vector of wheel center parallel with the tire-terrain contact plane
U	Velocity of the vehicle in the x-direction
$\vec{v}$	Velocity vector of the wheel center in the direction parallel to the tire-terrain contact plane

v

X	Vehicle longitudinal axis (forward is positive)
Y	Vehicle lateral axis (right is positive)
Z	Vehicle vertical axis (down is positive)
β'	Equivalent slip angle produced by camber effects
β	Tire slip angle (angle between $\vec{u}'$ and tire center plane)
φ	Tire camber angle
ψ	Steer angle of wheel (angle between $\vec{u}$ and the tire center plane)
Ω_T	Multiple of A_2 at which the assumed parabolic variations of small angle cornering and camber stiffness with tire loading are abandoned to preclude reversal in the sign of the side force under conditions of excess tire loading

Subscripts

f	Refers to the front wheels
r	Refers to the rear wheels
i	Refers to a particular wheel
	1 - right front
	2 - left front
	3 - right rear
	4 - left rear

LIST OF TABLES

LIST OF FIGURES

List of Figures
(continued)

INTRODUCTION

The mathematical description and numerical simulation of the motion of ground vehicles has been a goal of many researchers for some time. Since Broulhiet[1] first applied a theoretical analysis to study the shimmy problem, which eventually led to the standard use of independent front-end suspensions, many other vehicle handling and ride problems have been subjected to mathematical analysis. It was not until the late 1950's when a group of former aeronautical engineers at Cornell Aeronautical Laboratories[2] under Milliken, made a concentrated attack on the analysis of the entire vehicle that significant progress in understanding ground vehicle dynamics was made.

Segel[3] derived and validated a set of linear differential equations which described vehicle motion on a flat, smooth road in a straight, constant speed maneuver. This set was analyzed by the standard techniques of linear systems analysis and the results pinpointed the tires as one of the major influences in lateral motion and stability. Simultaneously, the theoretical analysis of the tire itself had been under study by many researchers, culminating in the development of a model described by Fiala.[4] His work defined and showed the importance of the slip angle concept of tire force generation. Tire descriptions and research, based on Fiala's model, are now generally accepted. Subsequently, other researchers discovered other parameters involved in tire force generation; namely, those related to camber and self-aligning torque. The vehicle model postulated

and validated by Segel required forces due to all three sources: slip angle, camber angle and self-aligning torque.

It was not until the middle 1960's that sufficient progress was made on the analysis of enough parts of the automobile that a simulation extending vehicle motion into the non-linear regime could be attempted. Again, it was engineers at Cornell, (McHenry and Deleys[5]) who compiled the available information and attempted to make it mutually compatible. In the process, the vehicle tires resumed their dominant role in the generation of forces. However, it became apparent that the available tire data did not encompass the entire range of anticipated motion. In particular, although data was available on side force due to slip angle alone and camber angle alone, not enough was known to specify completely the lateral forces generated when tires were run with <u>combined</u> slip and camber angles.

Based on their extensive experience in the analysis and testing of vehicles and tires, McHenry and Deleys postulated a tire force model which appeared eminently reasonable and was, in fact, validated in some full-scale tests with civilian passenger-car highway-type tires. This model postulated that the side forces generated by tires run at a camber angle could be approximated, for analytical purposes, by adding an additional slip angle to that which actually existed. This added angle is called the "equivalent slip angle" or that slip angle which would yield a side force "equivalent" to that generated by the angle of camber.

Since military tires, however, have a radically different tread design and cross-sectional profile than do civilian tires, this study was undertaken to determine the applicability of McHenry and Deleys' model to military tires and to obtain a better understanding of the performance of military tires at combined slip and camber angles as an aid to the design of future military vehicles. Therefore, the main purposes of this study were to:

1. Test the applicability of the McHenry and Deleys' mathematical model of camber angle as an equivalent slip angle to military tires and,

2. Generate test data for the 7.00-16 NDCC military tire.

A review of the theory and material pertinent to the elements of tire dynamics is presented prior to a description of the experimentation accomplished.

BACKGROUND

1. General

The vehicle and its operator are knitted together into a con-
trolled moving unit by the brake and accelerator for velocity changes
and by the steering mechanism for vehicle control. Each of these man-
machine interactions affect vehicle stability, and the investigation
of the combinations of both would cover the entire range of vehicle
stability. The scope of this study, however, will be limited to tire
dynamics resulting from steering wheel deflection; consequently,
braking and tractive effects are neglected.

It is obviously desirable that a wheel undergoing maneuvers
maintain a rolling motion. Considering Figure 1. When the tire is in
a pure rolling mode, its velocity vector, $\vec{u}$, lies in the plane of the
wheel, parallel to the X-axis. The wheel plane (the XY-plane) is
normal to the road. However, the tire could be propelled in a pure
skidding mode. In this case, its velocity vector would be normal to
the wheel plane, parallel to the Y-axis. If the velocity vector of
the wheel has components in both of these directions, the tire is both
skidding and roll'ng. It is this combined situation which generates
vehicle stability and control forces and with which this study is
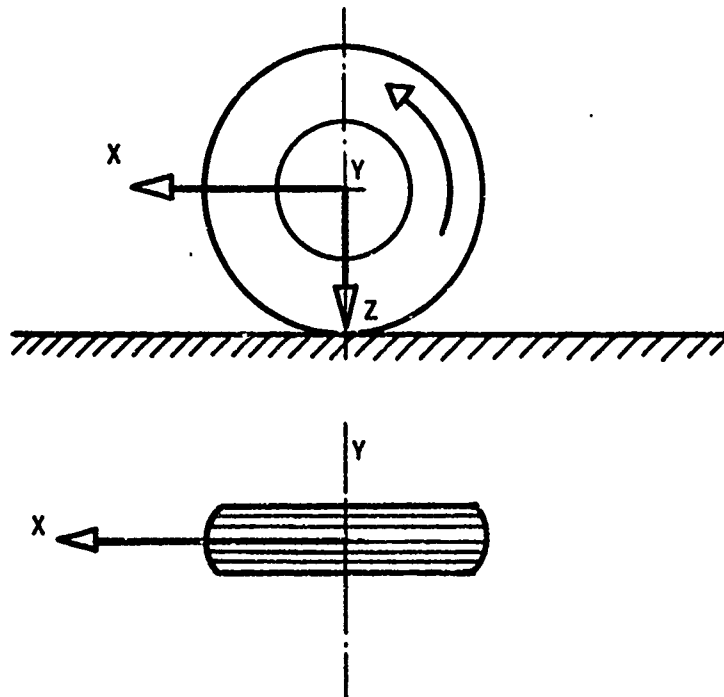primarily concerned.

FIGURE 1. ROLLING TIRE, SIDE AND TOP VIEWS[2]

2. Steering Dynamics

An introduction to the field of tire dynamics would be incomplete without the mention of slip angle and the generation of lateral cornering forces and self-aligning torque. The tire is a dynamic body. Dependent on interacting design parameters, it not only rolls along the road, but also bends and flexes under load changes caused by surface irregularities and weight transfer within the supported vehicle. Consequently, it does not necessarily roll along the direction indicated by the intersection of the wheel plane and road surface, but may take some different course. The angle formed between the plane of the wheel and the plane of some imaginary wheel rolling along the path actually taken, is called the "slip angle." Referring to Figure 2, this angle is shown as β_f and β_r for the front and rear wheels, respectively.

How this angle actually arises can be seen from the following discussion. In order for a vehicle to deviate from a straight line, and external force must be provided. This force can only be provided by the tires. Once into the turn, the vehicle is subjected to a centrifugal force which would cause the vehicle to travel along a tangent to its path of motion. This centrifugal force is countered by tire generated centripetal forces. These forces (shown as F_{s_f} and F_{s_r} in Figure 2) cause the tire-ground contact patch to distort so that the rolling tire plane is at an angle to the direction of motion of the wheel center, $\vec{n}$. Conversely, if the driver introduces to the wheel a steering angle, ψ, oblique to the direction of vehicle motion,
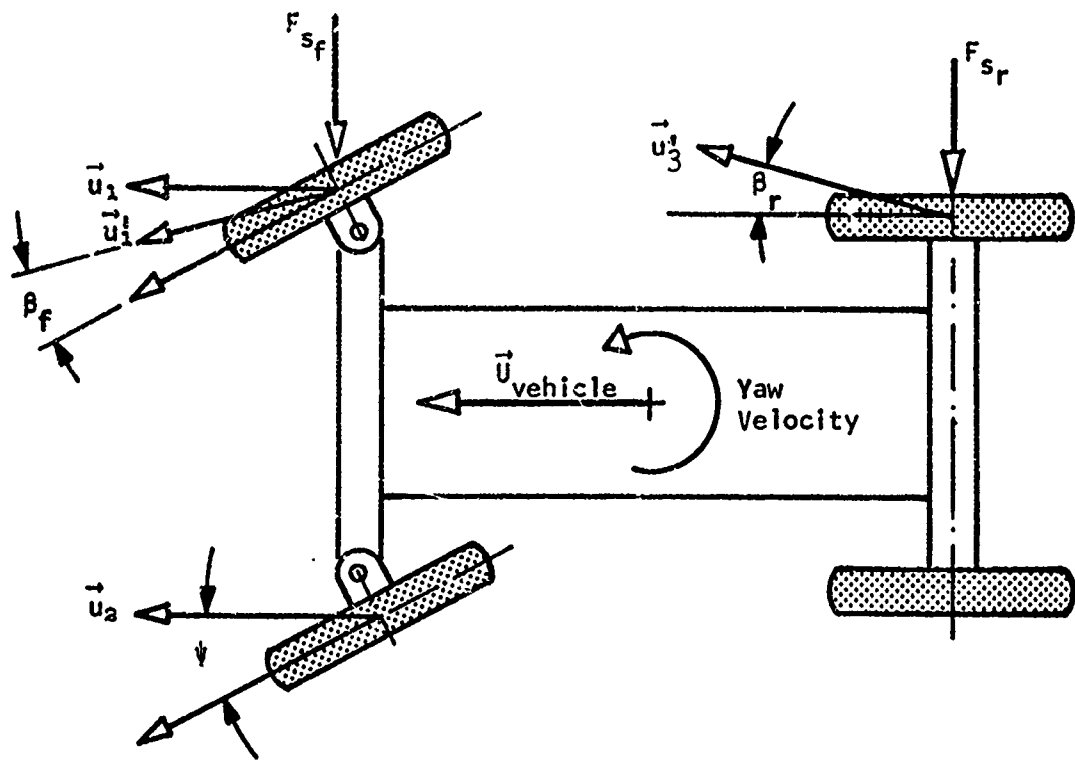
a. Vehicle Entering Turn
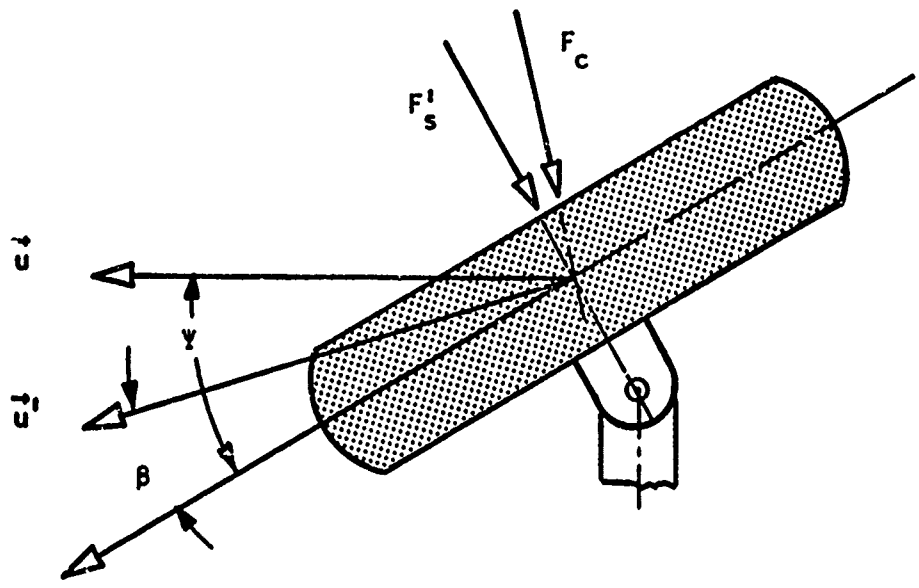
b. Front Wheel During Turn

FIGURE 2. DIAGRAM OF A VEHICLE DURING A TURNING MANEUVER[7]

the tire will develop a distortion that will generate between the tire-road interface side forces and turning moments.

With the steering angle held constant, the wheel center velocity changes to a new vector, $\bar{u}'$, with the angle between $\bar{u}$ and $\bar{u}'$ less than the steering angle, ψ. When $\bar{u}'$ is established, a slip angle, β, is said to prevail. That the slip angle is less than the steering angle is a consequence attributable to tire elasticity. This phenomena will be discussed further, but it should be noted here that the term "slip angle" is a misnomer since the tire actually stretches or creeps rather than slips. Also, note that, due to the angular yaw velocity that is taken by the vehicle, the rear tires also develop a slip angle and corresponding cornering forces.

Referring now to Figure 2b, at this juncture the side thrust F_s has changed direction by the slip angle β_f, and is denoted as F_s'. The force F_c, called "cornering force", is introduced and is the component of F_s, lying in the plane of the tire contact patch, and normal to the new velocity vector, $\bar{u}'$. Note that at zero slip angle $F_s = F_c$, since the new velocity vector and the old are the same.

3. Cornering Force and Camber Thrust

The cornering force has been introduced as a lateral force in the tire-terrain contact plane, perpendicular to the wheel velocity vector. The existence of the cornering force is attributed to the elastic properties of the tire, and is present only when a slip angle prevails, i.e., when the wheel's velocity vector does not lie in its plane.

Figure 3a depicts a tire turned through a steering angle, ψ, greatly exaggerated in this figure for clarity. Now imagine the movement of an incremental element of tire as it travels through the contact patch. For simplicity of discussion, assume that there is no tire distortion before road contact and that the road is parallel to the vector u so that $\vec{u} = \vec{u}'$.

Initially, the tire element contacts the road at point 1 which is on the wheel center plane AB. As the wheel rotates and moves along vector $\vec{n}'$, the contact element must move to points 2, 3, 4 and 5, unless it slips along the road surface. The wheel center plane, however, remains along line AB, hence the tire must be distorted by the distance 2a, 3b, 4c and 5d.

The resultant of these incremental distortions in the tire-road interface is the tire force, F_s. Since there is greater distortion at the rear of the contact patch, this resultant is rearward of the wheel center, thus generating a moment about the wheel center called the "self-aligning torque." F_s can be resolved into two components: F_c, the previously mentioned cornering force normal to the wheel
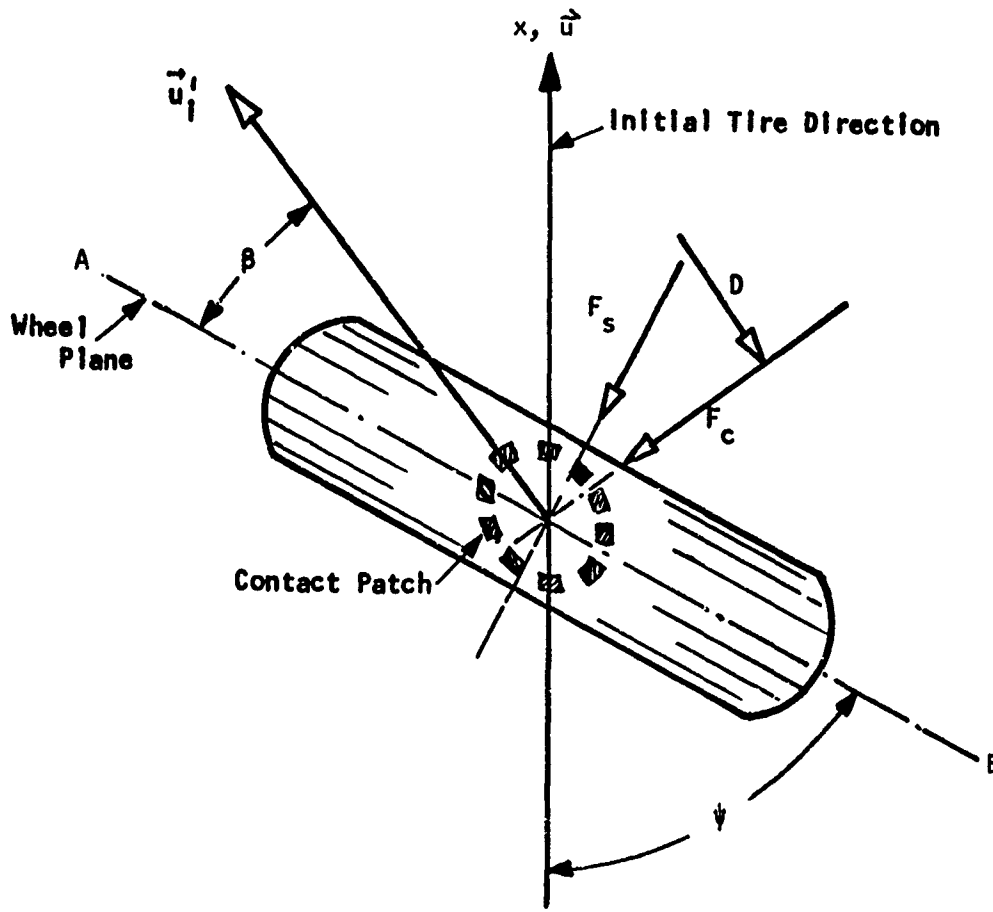
a. Comparison of Steering Angle, ψ and Slip Angle, β
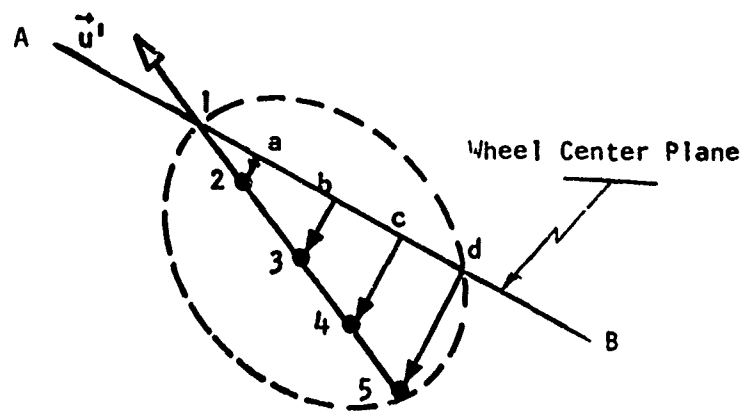
b. Schematic of the Tire Contact Patch
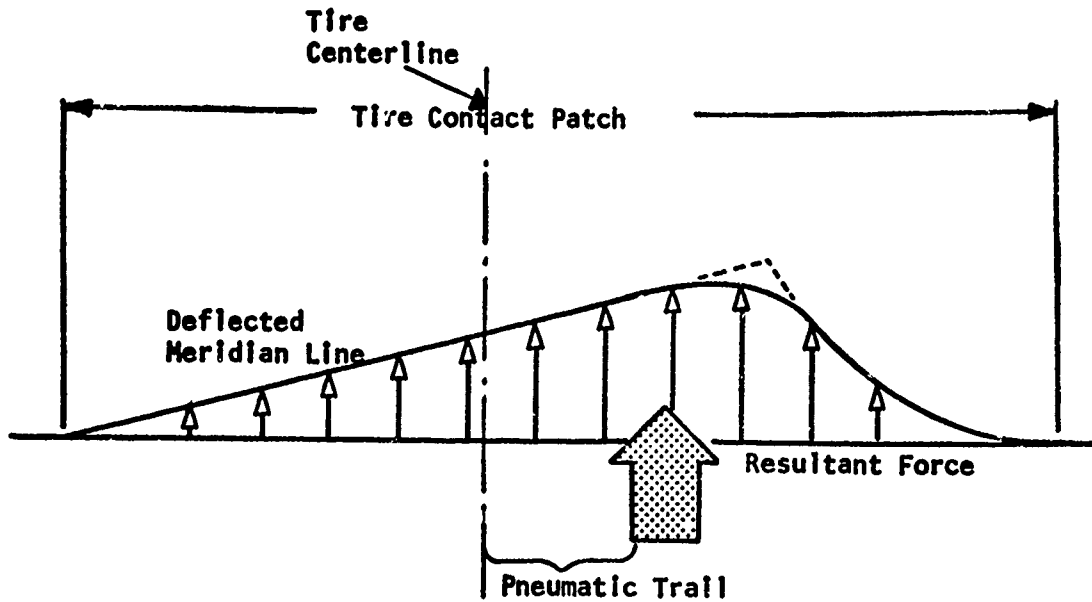
FIGURE 3. SCHEMATIC OF A STEERING TIRE[2]

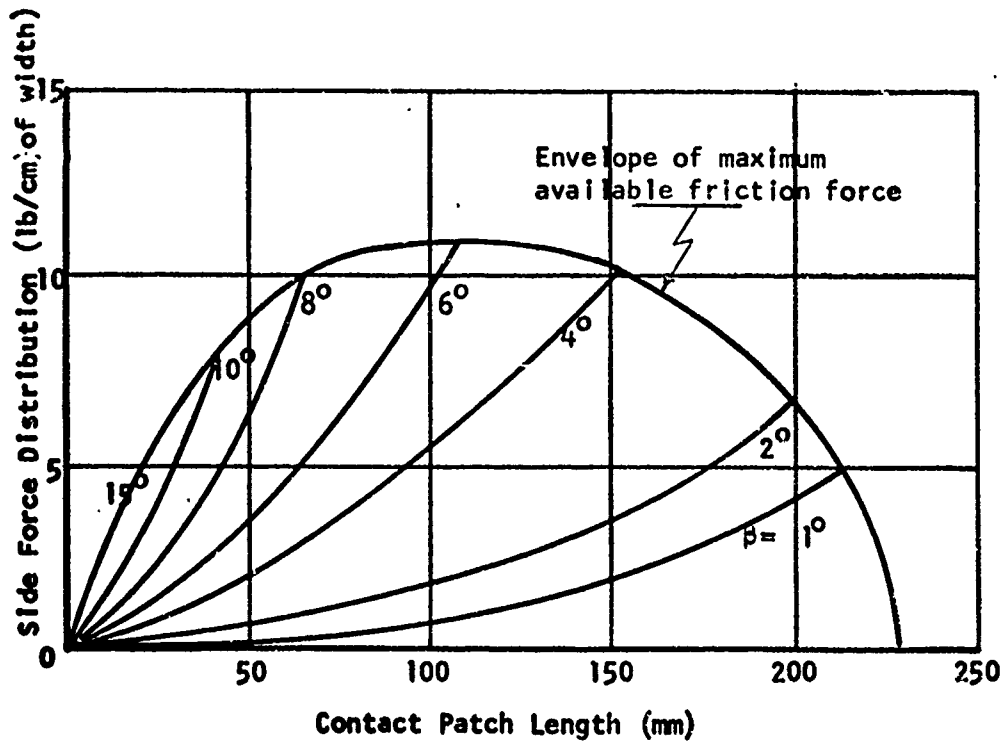**FIGURE 4. TYPICAL PLOT OF TIRE SIDE FORCE, SHOWING HOW THE PNEUMATIC TRAIL IS GENERATED.**

FIGURE 5. TYPICAL SIDE FORCE DISTRIBUTION IN THE CONTACT PATCH OF A PASSENGER CAR TIRE, WITH DIFFERENT SLIP ANGLES, β [3]

center velocity $\vec{u}$, and D, parallel to u, a drag force opposing tire
motion and, consequently, acting as an additional rolling resistance.
Thus, more power is needed to maintain steady-state motion in a turn
than is required in straight-ahead motion.

Contrary to the simplified presentation of Figure 3, the lateral
force, F_s, is not a maximum at the very end of the contact patch. As
the tire element moves through the contact patch, the pressure steadily
increases to a maximum and then decreases to zero due to the rotation
of the wheel and the initially circular shape of the tire. Thus at
some point the tire-road frictional bond becomes less than the stress
caused by distortion. At that point the bond will break, causing tire-
road sliding and force deterioration. This situation is depicted
graphically in Figure 4.

Figure 5 shows a plot of side force distribution versus contact
patch length for various slip angles. The circular curve represents
the envelope of maximum available tire-road friction due to the tire
contact pressure and the tire-road coefficient of friction. The area
under any curve is the total side force developed at that angle of
slip, and the first moment of this area about the center of the contact
patch is the self-aligning torque.

A convenient parameter is called the "pneumatic trial." This
is the imaginary distance behind the wheel center where all the side
force may be considered to be concentrated. This distance may be
calculated by dividing the self-aligning torque by the total side force.
The self-aligning torque and the moments caused by the designed caster

angle must be opposed by the steering mechanism. These moments also cause the wheel to return to the straight-ahead direction when the steering wheel is released.

Figure 6 shows typical side thrust and self-aligning torque plots for various slip angles for a particular load on a given tire. The slope of the side force curve at $\beta = 0$ is called the "cornering coefficient" or the "cornering stiffness" and is one of the most important parameters of a tire in vehicle motion simulation and analysis.

If we increase the load on the tire, initially we get an increase in cornering force, as would be expected. However, as the load increases, the tire patch area increases at a greater rate so that the tire contact pressure actually decreases. This decrease in pressure causes the tire-road friction bond to fail further and further forward so that, eventually the side force reaches a maximum and then begins to fall off with increasing load. A typical plot of side force verses load for various slip angles is shown in Figure 7.

In addition to the side force generated by tire slip angle, tires also generate a side force if the plane of the wheel is not perpendicular to the plane of the road (see Figure 8). This force is called "camber thrust," and is in the same direction as the camber angle, φ.

Camber angle between the tire and road are designed into the vehicle. However, with changing roll angle and suspension deflection, this angle may also change, yielding significant variations in camber thrust during a dynamic maneuver.
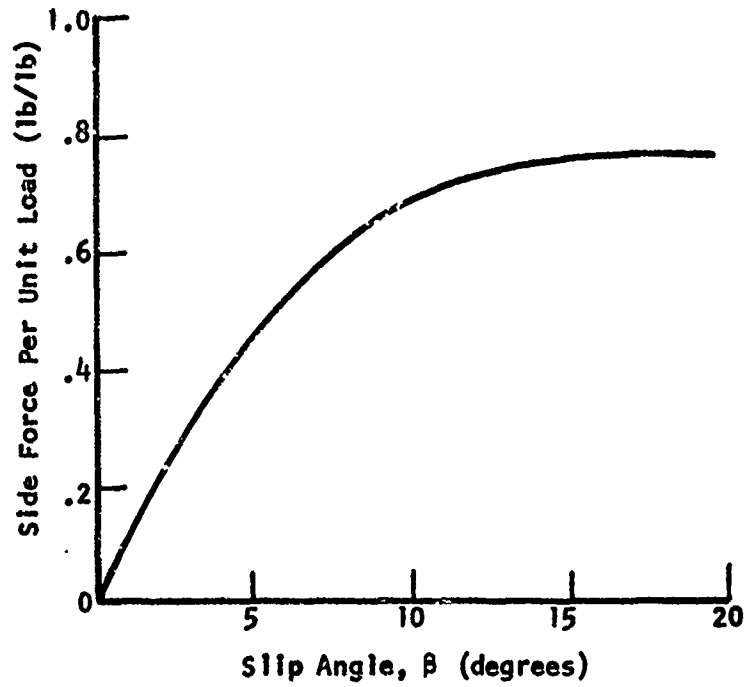
a. A Typical Side Force vs Slip Angle Plot
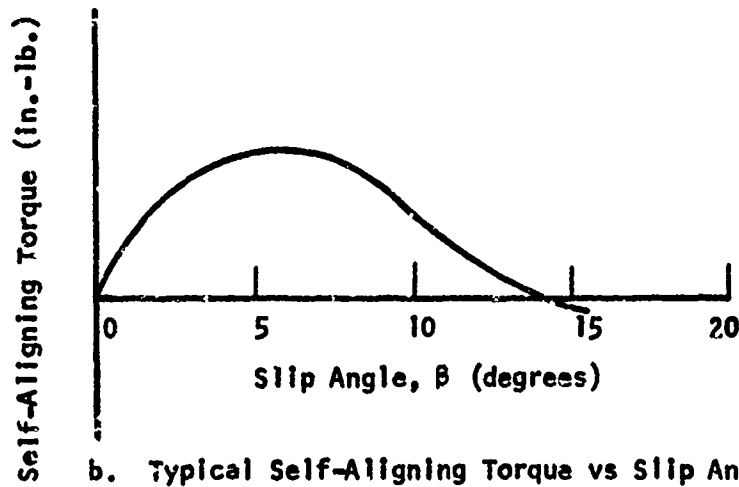
b. Typical Self-Aligning Torque vs Slip Angle
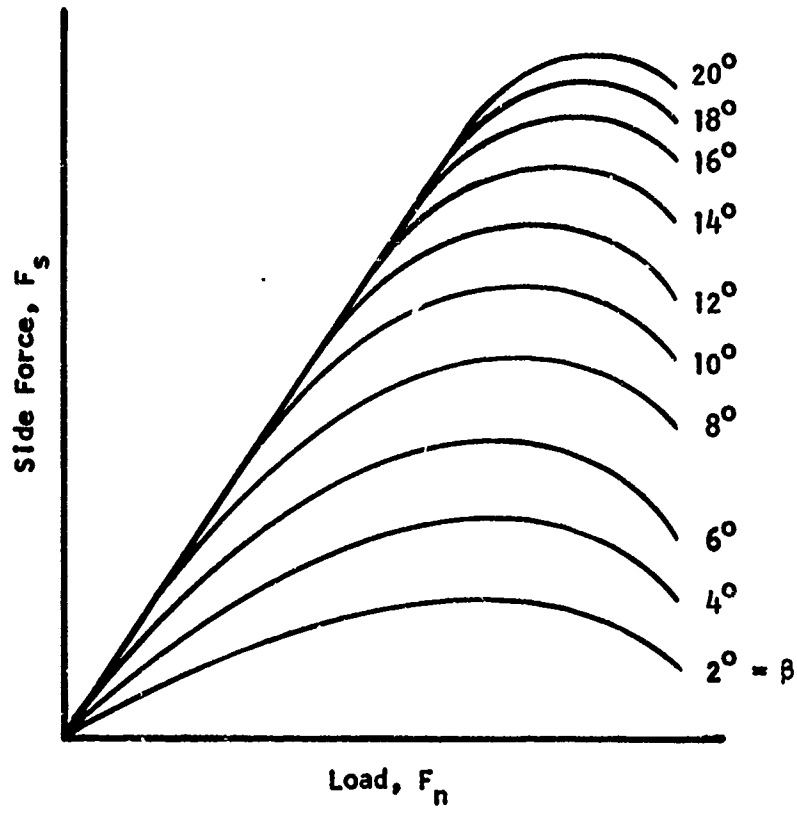
FIGURE 6. TYPICAL TIRE CHARACTERISTIC PLOTS[4]

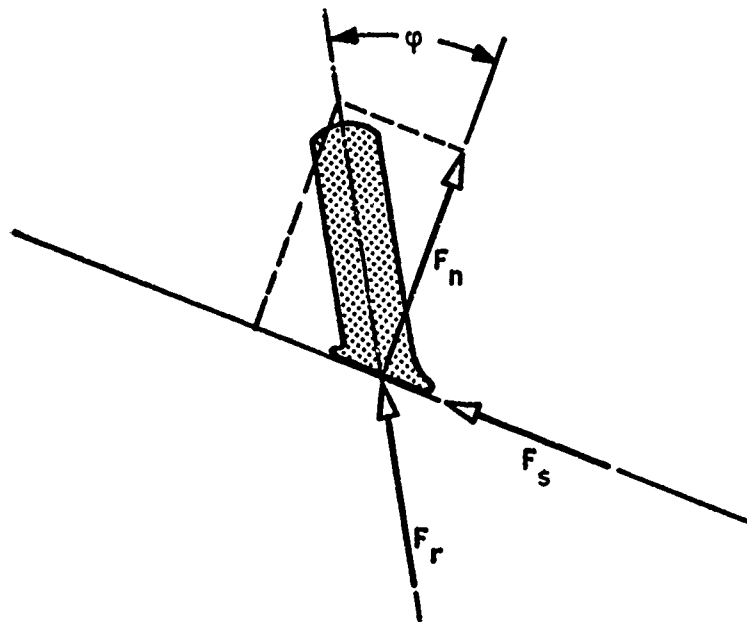FIGURE 7. TYPICAL SIDE FORCE VS LOAD PLOT
FOR VARIOUS SLIP ANGLES[4]

FIGURE 8.

PORTRAYAL OF A PNEUMATIC TIRE
AT A CAMBER ANGLE TO THE ROAD[1]

4. Cornering Theory

McHenry and Deleys[5] postulated that the total side force deve-
loped by a tire on which a camber angle is imposed during a cornering
maneuver, can be represented analytically by combining the force
generated by the actual cornering slip angle with an additional incre-
mental slip angle, called the "equivalent slip angle" to be used to
account for camber thrust. This total angle, in combination with
pressure, load and other pertinent tire parameters, could then be
utilized to predict total side force. Their development of this
concept is presented below for completeness.

In Figure 8, let F_o be the radial loading of the tire, i.e.,
the load applied parallel to the plane of the tire, through its axis.
This loading is dependent only on the suspension deflection and the
tire dynamics and is independent of the tire position with respect to
the local terrain. The tire-terrain contact point (which is actually
an area) is defined as the intersection of the terrain plane, the
wheel plane, and a plane through the wheel axis, normal to the terrain.

From the radial force, the normal force F_n, the component of F_o
perpendicular to the road plane, on which side, traction and braking
forces depend, can be calculated. The total side thrust, F_s, including
both the effects of camber thrust and slip angle, is the component of
F parallel to the ground plane. Applying statics, instantaneously,
with no vertical or lateral accelerations, and considering only forces
perpendicular to the tire plane

$$F_o = F_n \cos\varphi + F_s \sin\varphi \tag{1}$$

or

$$F_n = F_n \sec\varphi - F_s \tan\varphi \tag{2}$$

Thus, with the radial load and camber angle known, the normal load and side thrust can be determined.

As mentioned before, small angle cornering stiffness, C_{so} is defined as the partial derivative of the side force with respect to slip.

McHenry and Deleys[5] observed that a plot of cornering stiffness versus tire normal load can be approximate by a parabola such as shown in Figure 9. Thus

$$C_{so} = \left. \frac{\partial F_s}{\partial \beta} \right|_{\beta=0} = A_o + A_1 F_n - \frac{A_1}{A_2} F_n^2 \tag{3}$$

$$= \frac{-A_1 F_n (F_n - A_2) + A_o A_2}{A_2} \tag{4}$$

Here, A_o, A_1, and A_2 are coefficients of the parabola chosen to obtain the desired fit to measured data.

In a similar manner, they postulated that camber stiffness, the partial derivative of camber thrust with respect to camber angle, measured at zero camber angle, can also be approximated with a quadratic:

$$C_{co} = \left. \frac{\partial F_s}{\partial \varphi} \right|_{\varphi=0} = A_3 F_n - \frac{A_3}{A_4} F_n^2 \tag{5}$$

$$= \frac{A_3}{A_4} F_n (A_4 - F_n)$$

Again, A_3 and A_4 are constants achieving the best fit to measured data (see Figure 10).

Under extreme loadings, the data for both cornering and camber stiffness are no longer parabolic, but appears to level off. The loading at which this occurs is given the value $\Omega_T A_2$, where, usually, $0.80 < \Omega_T < 1.15$ and A_2 is the coefficient of Equations (3) and (4).

The concept of a non-dimensional slip angle can now be developed to generate the equivalent slip angle to be used in the approximation of camber angle effects.

Assuming zero traction and braking, the side forces generated at small slip angles can be written as:

$$F_{ss} = C_{so}\beta \tag{6}$$

$$F_{ss} = \left[\frac{-A_1 F_n (F_n - A_2) + A_o A_2}{A_2}\right]\beta \tag{7}$$

If the forward velocity of the wheel is u and the transverse velocity is v, then the slip angle of the tire, β, is not the steering angle, ψ, but

$$\beta = \psi - \frac{v}{u}$$

Therefore:

$$F_{ss} = \left[\frac{-A_1 F_n (F_n - A_2) - A_o A_2}{A_2}\right]\left(\frac{v}{u} - \psi\right)$$

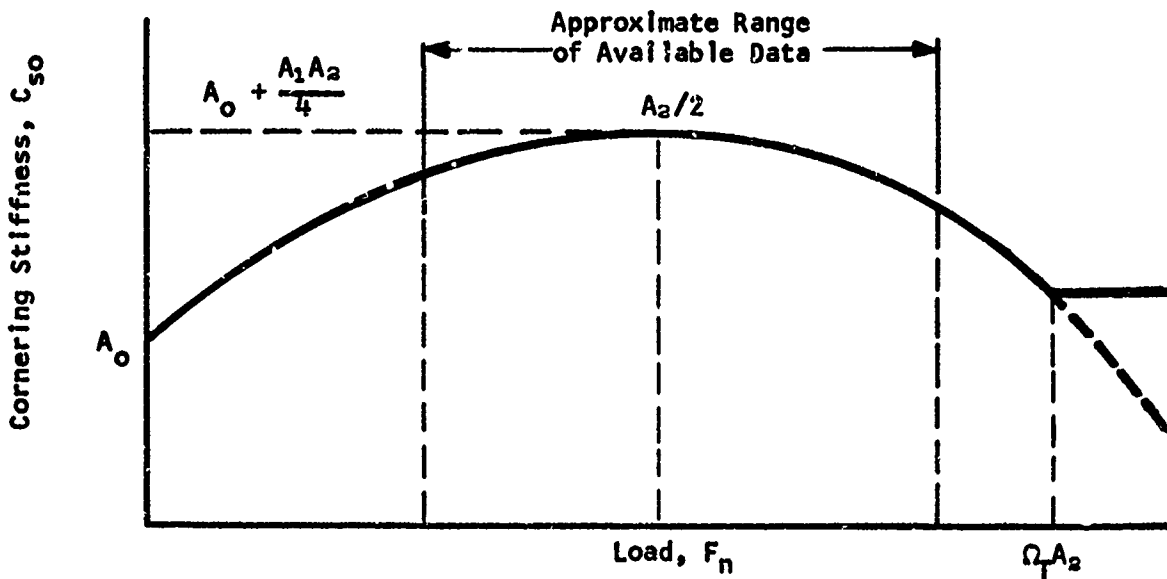and the side force generated by small camber angles can be written as:

FIGURE 9. TYPICAL PLOT OF CORNERING STIFFNESS VS LOAD[1]
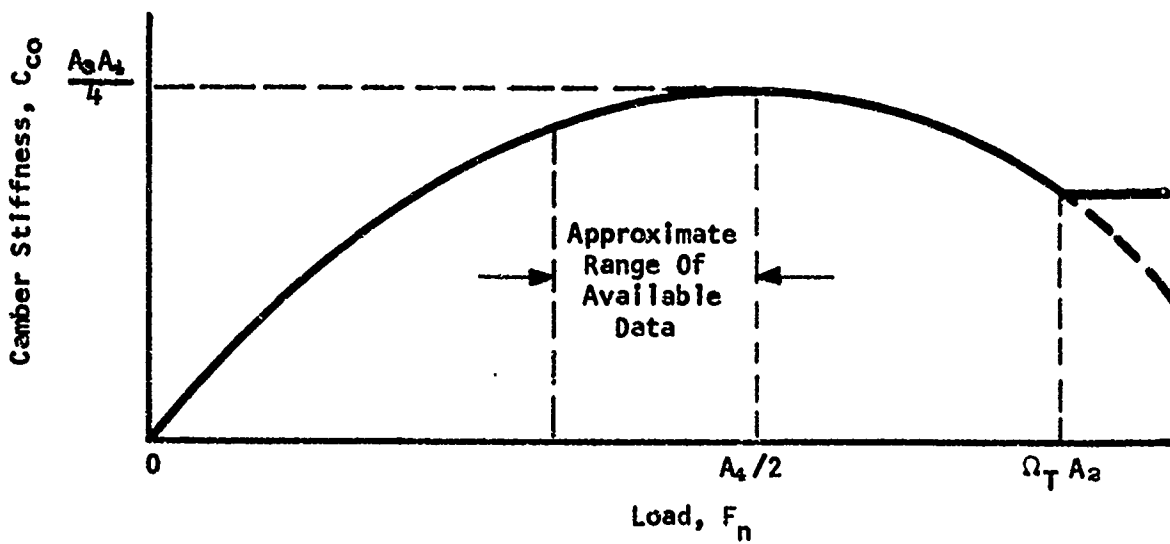
FIGURE 10. TYPICAL PLOT OF CAMBER STIFFNESS VS LOAD

$$F_{sc} = C_{co}\varphi \qquad (8)$$

$$= -\left[\frac{A_3}{A_4} F_n(F_n - A_4)\right]\varphi \qquad (9)$$

Because of unavailable data for large camber angles, McHenry and Deleys assumed that the camber thrust under a constant normal load reaches its maximum at $\varphi = 45^\circ$. Accordingly, a parabolic relation of camber force to camber angle was adopted, as shown in Figure 11. Equation (8) can then be modified to the following form which covers all camber angles from 0 to $\frac{\pi}{2}$:

$$F_{sc} = -\left[\frac{A_3 F_n(F_n - A_4)}{A_4}\right]\left(\varphi - \frac{2}{\pi}\varphi|\varphi|\right) \qquad (10)$$

FIGURE 11. ASSUMED CAMBER THRUST VS CAMBER ANGLE[B]

For $\varphi = \pm \frac{\pi}{4}$, $(\varphi - \frac{2}{\pi} \varphi |\varphi|) = \mp \frac{\pi}{8}$, and the maximum camber thrust as a function of normal load is given by:
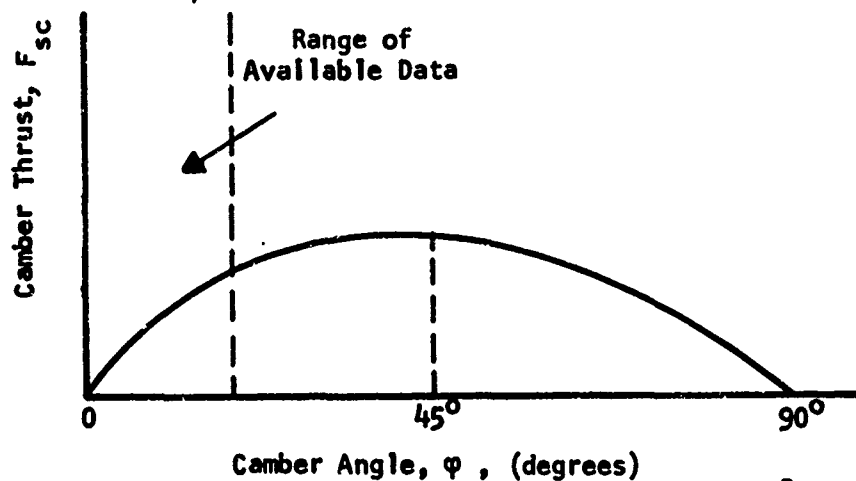
$$F_{sc_{max}} = \pm \left[\frac{A_3 F_n (F_n - A_4)}{A_4} \right] \frac{\pi}{8}$$

Note, that for $\varphi = 0°$, $\pm 90°$, $F_{sc} = 0$.

Milliken[8] assigns an angle β' which, for small angles will give the same side force as the camber angle, φ. β' is called the "equivalent slip angle" which, from Equation (6):

$$F_{sc} = C_{so}\beta' \tag{10}$$

But, from Equation (8):

$$F_{sc} = C_{co}\varphi \tag{8}$$

Therefore, for small angles

$$\beta' = \frac{C_{co}}{C_{so}} \varphi \tag{11}$$

and, from Equation (10), for larger angles

$$\beta' = \frac{C_{co}}{C_{so}} (\varphi - \frac{2}{\pi} \varphi |\varphi|) \tag{12}$$

Thus, the total side force resulting from small slip angles and the entire range of camber angles is

$$F_s = F_{sc} + F_{s_s} = C_{so}(\beta + \beta') \tag{13}$$

The purpose of this study is to conduct an experimental program to assess the validity of Equation (12) as it pertains to the U. S.

Army NDCC military tire used on 1/4-ton trucks. In other words, is the side force generated by camber angle independent of slip angle?

EXPERIMENTAL PROGRAM

1. Program Philosophy

When considering methods for the measurement of tire forces, it would seem obvious to measure tire loads while the tire is operating on a vehicle. However, tire performance invariably includes effects due to the vehicle suspension, its mass, and operator controls. Consequently, for this study the tires were placed on the wheels of an unsprung trailer, thereby eliminating the effects due to both operator and suspension, yet still retaining tire-terrain contact and the resulting interaction. This specially-designed trailer allowed for variation of camber angle simultaneously with slip angle, normal load, and, of course, tire pressure. Since the inputs to McHenry's lateral force expressions consist of normal load, camber angle, slip angle, cornering stiffness and camber stiffness, this trailer lends itself well to the problem under investigation while maintaining simplicity in testing.

Data was obtained for the military 7.00-16 NDCC tire, which is used on the 1/4-ton truck. Forces were measured at 3 miles per hour, for steady state slip angles up to 10 degrees. Camber angle and tire normal load were also varied. Testing was accomplished, by the author, during August and September of 1970 and resulting in the accumulation of over 800 data points.

2. Test Apparatus

The trailer utilized in this study is shown in Figures 12 and 13. It consisted of a functional T-frame, devoid of suspension. The axle shafts were pivoted about a vertical kingpin to induce toe-in or toe-out of the tires. This rotation was controlled by a telescoping tie rod in the form of a double-ended jack screw; the angle of toe-in was equal for both tires. The jack screw was transversely fixed to the frame and was turned by a reversible electric motor controlled through an umbilical cable from the prime mover. A linear potentiometer and a large protractor, used for visual observation and calibration, indicated the toe-in angle of the tires with respect to the trailer longitudinal centerline.

The tire camber angle was varied from -2 degrees to +8 degrees by inclining the kingpin. An extra wheel trailing to the rear along the trailer frame centerline connected through an angular potentiometer measured trailer yaw relative to the direction of travel. This extra wheel is called a "Beta" wheel.

Side thrust generated by each tire was transmitted axially through the wheel hub to a load cell mounted directly behind the sub-axle of each wheel. Free floating wheel bearings permitted freedom of movement, although several wheel revolutions under a particular lateral load were necessary to allow equilibrium to ensue. Since both tires were yawed at equal, but opposite angles, the side forces developed must be equal, but opposite. Measuring both tires, therefore, was a redundancy. If one tire produced a greater side force than the

other at the imposed angle, the trailer would develop a yaw angle, thereby reducing the slip angle of the former tire and increasing that of the latter, thereby equalizing the forces. Thus the need for a Beta wheel.

. The prime mover employed during the test was a 1969 Chevrolet C-20 Suburban Station Wagon. The vehicle housed all control and recording equipment. The vehicle had sufficient power to maintain constant velocity against the heavy drag imposed during large normal tire loads and slip angles. The control panel was mounted so that the test operator could view the large toe-in protractor mounted on the trailer. The panel provided the switches needed to activate the data recorders and to set the toe-in angle.

Two strip chart oscillographs recorded tire side thrust, as measured by the load cells behind the stub axles; trailer yaw, measured by the fifth wheel angular potentiometer; and toe-in angle of the tires, as measured by an angular potentiometer. Both recorders were of the same type and used carrier amplifiers giving an internally generated excitation voltage. Thus, they were capable of measuring outputs from either active AC or passive DC transducers and reflected outstanding stability and repeatability when used with resistance type strain gauge bridges. To reduce drift, the amplifiers were given a 15 minute warm up period before each day of testing, and were left on throughout the test day. The 115 volt AC power required by the recorders was supplied by an inverter operating off the vehicle battery.
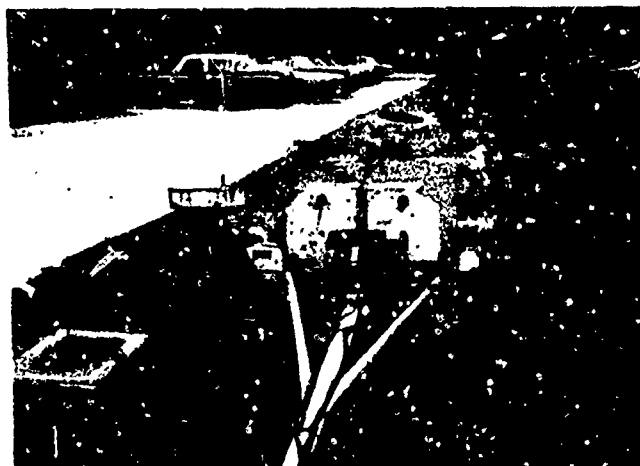
FIGURE 12. "TOE-IN" TRAILER

FIGURE 13. CLOSE-UP OF TIRE AT HIGH SLIP ANGLE

A load cell indicator was used to measure the weight on the trailer tires and to calibrate the tire side thrust load cells.

3. Test Procedure

A pair of new 7.00-16 NDCC tires were mounted on the toe-in trailer and balanced. Since the majority of accidents with the vehicles using these tires had pressures in the 24 to 28 psi range, and since preliminary tests indicated that pressures near 28 psi yielded comprehensive data most applicable to the McHenry analysis, the test program was run with the pressure maintained at 28 psi. This pressure was checked each day prior to initiation of testing.

Initially, calibration procedures were extremely time consuming. With experience gained by repetition, the time required to calibrate was reduced to approximately two hours before testing each day. After calibration, the trailer was towed from the static test area about a quarter of a mile to the test site, a parking lot at Stevens Institute of Technology.

Each camber angle test used ten to twelve different slip angles, each with loads of approximately 500, 700, 900, 1100 and 1300 pounds per tire. The camber angles used were $0°$, $+2°$, $+4°$ and $+6°$ (positive camber angle indicates that the tire plane slants outboard of the vehicle, from bottom to top). The slip angles used were from $-1°$ to $+10°$ in one degree increments (positive slip indicates toe-in).

For a given camber angle and load, measurements were made for each slip angle. To insure steady-state conditions, each test was run for a distance of 100 feet. The load was changed after each series of slip-angle runs and the series repeated. During all test periods, the weather was clear or partly cloudy with temperatures ranging from

75° to 85°. No corrections were made for deterioration of tires or change of pavement conditions during the test. Tire wear was noticeable but slight, and it was assumed it would have no influence on the validity of the subsequent data analysis. It became evident, however, that there exists a need to study the effect of tire wear on lateral force generation.

All tests were conducted at approximately 3 mph, based on the study by Nothstine and Beauvais[9] of Ford Motor Company, which indicated that side forces are rather independent of velocity on dry pavements (see Figure 14). However, in tests conducted on wet pavement, by Kamm and Starrett of the Davidson Laboratory[10] there was a definite reduction in side force as velocity was increased. Therefore, all tests were conducted on dry pavement.
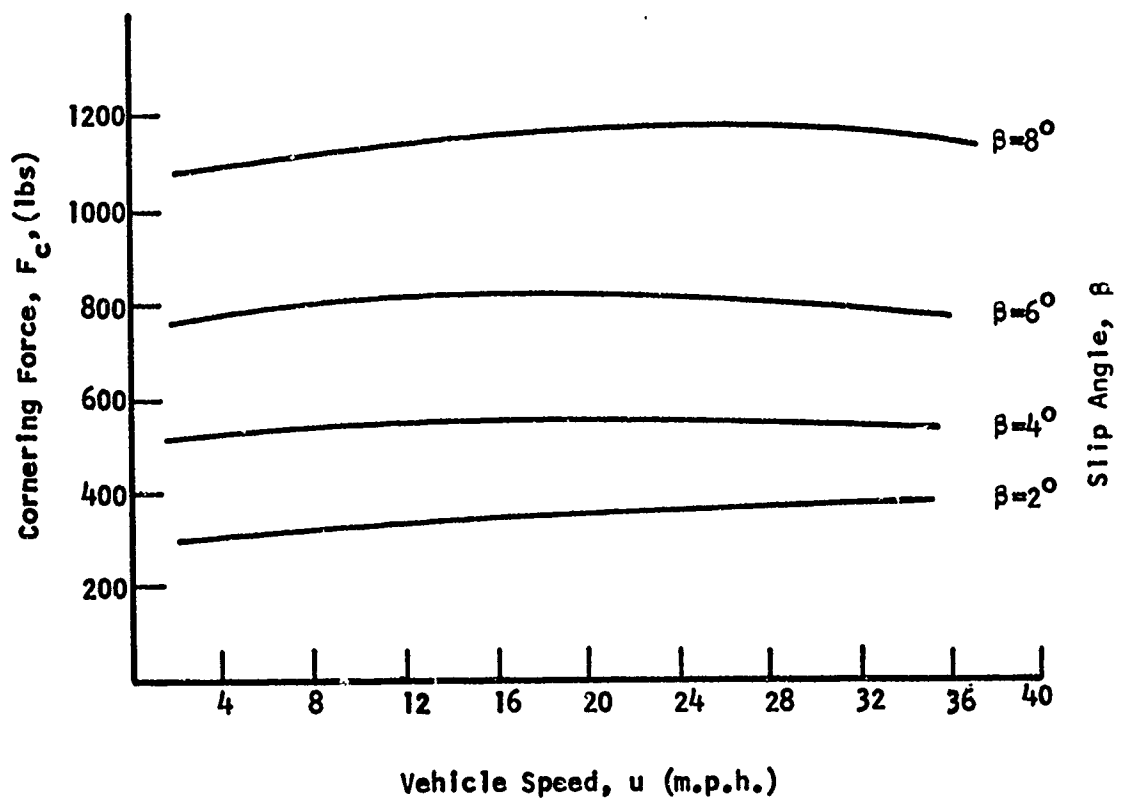
FIGURE 14. EFFECT OF SPEED ON CORNERING FORCE
FOR VARIOUS SLIP ANGLES[9]

4. Test Results

All results presented here are corrected for trailer yaw as measured by the Beta wheel. In the program, no yaw angles greater than 1.5° were measured. Figure 15 shows a typical plot comparing measured data and that corrected for trailer yaw.

Due to erratic performance of the left wheel load cell later attributed to a faulty bearing, only data measured on the right wheel is presented here.

Figures 16 through 20 depict measured side force versus slip angle at 0° camber at various normal loads. Their slopes at 0° slip define their respective cornering stiffness values, which are listed in Table 1 and plotted in Figure 21.

TABLE 1
Cornering Stiffness vs Normal Load from Figures 16-20

F_n (lb)	$\left. \dfrac{\partial F_s}{\partial \beta} \right\|_{\beta=0}$ (lb/deg)
490	75.5
700	111.0
905	130.0
1120	155.0
1310	138.0

By means of a least squares fit, the plot of Figure 21 may be approximated by the parabolic quadratic of Equation (4) using the following coefficients:
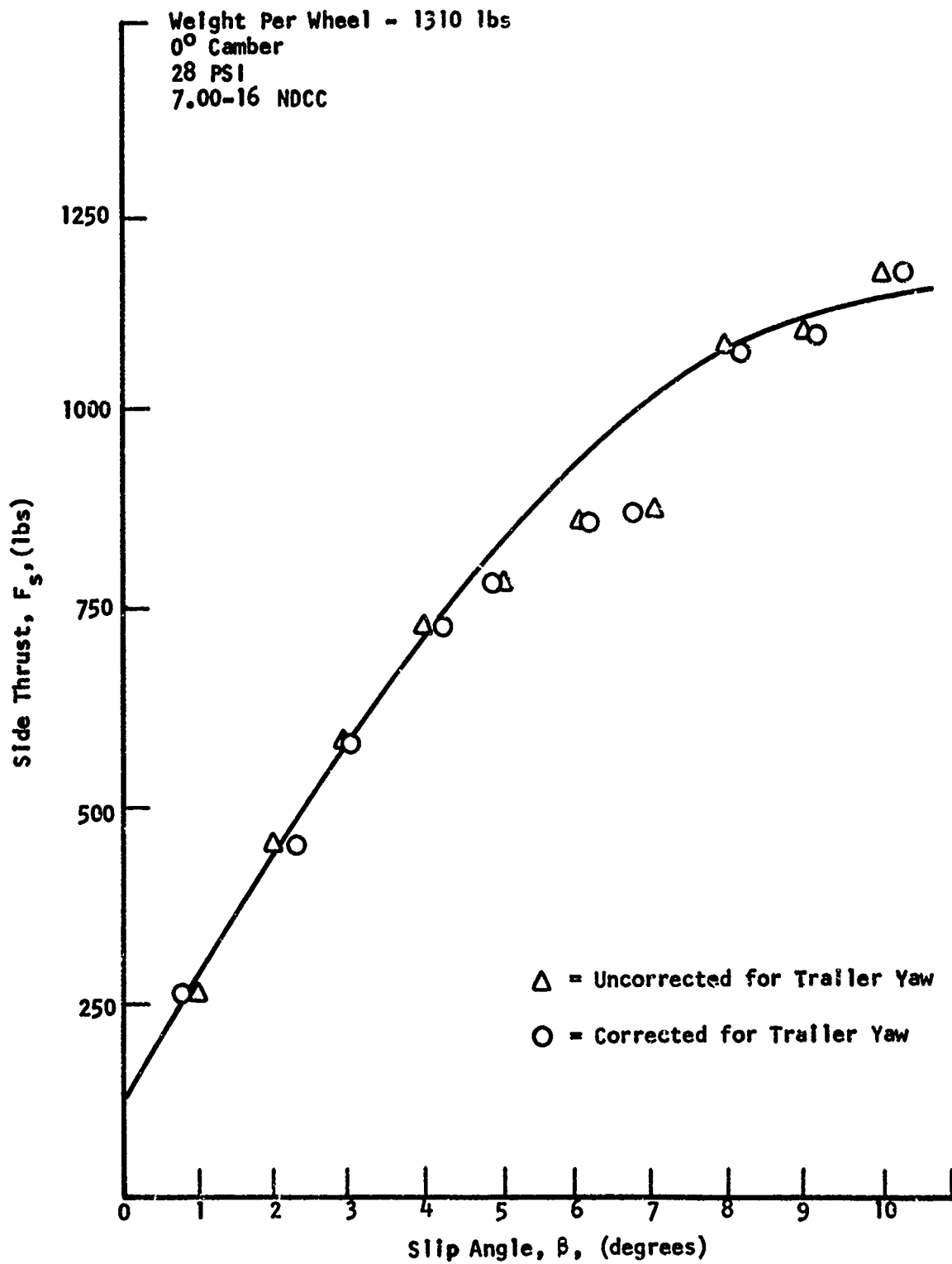
Weight Per Wheel - 1310 lbs
0° Camber
28 PSI
7.00-16 NDCC

$\triangle$ = Uncorrected for Trailer Yaw

$\bigcirc$ = Corrected for Trailer Yaw

Side Thrust, F_s, (lbs)

Slip Angle, β, (degrees)

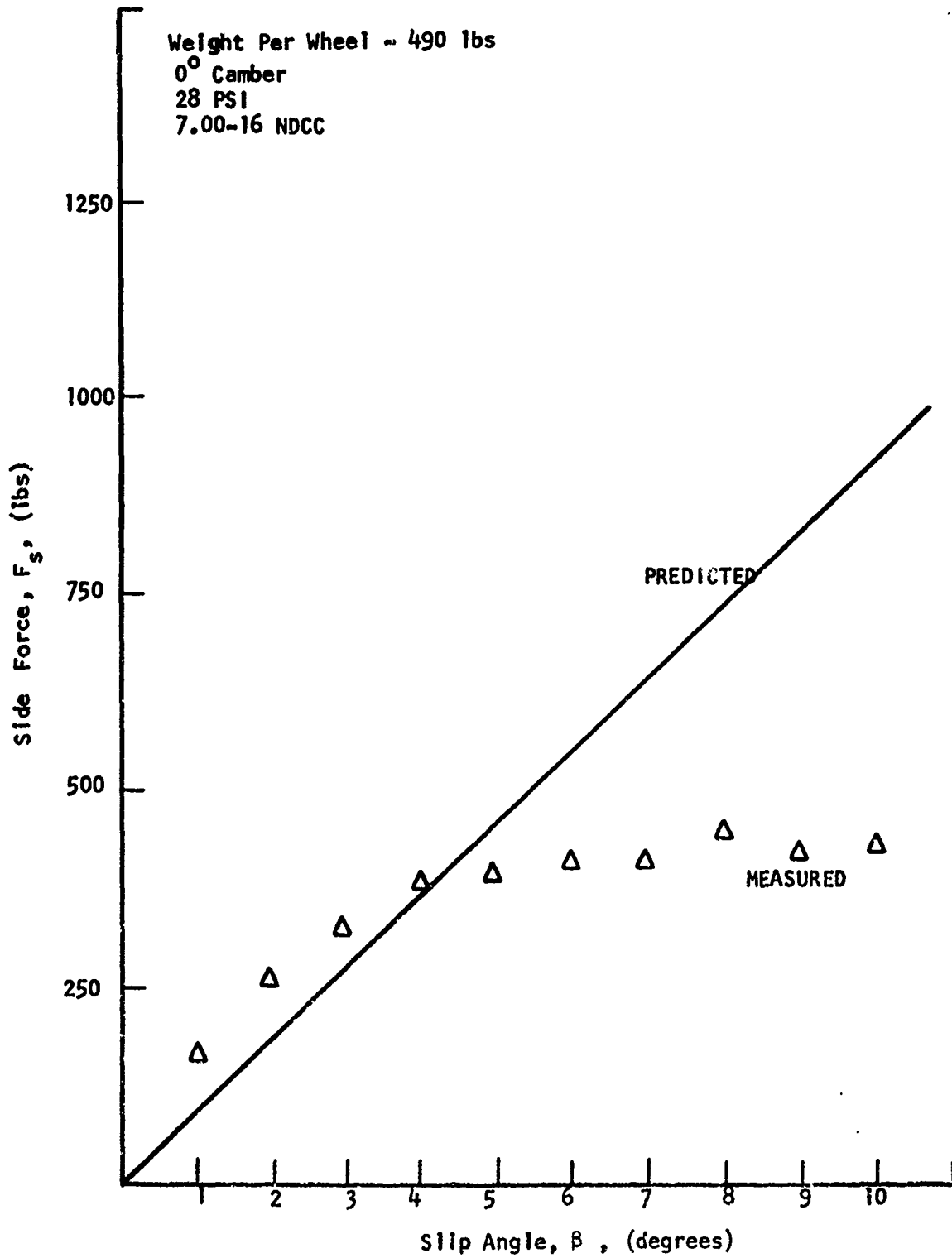FIGURE 15. EFFECT OF TRAILER YAW CORRECTION

FIGURE 16. COMPARISON OF MEASURED AND PREDICTED
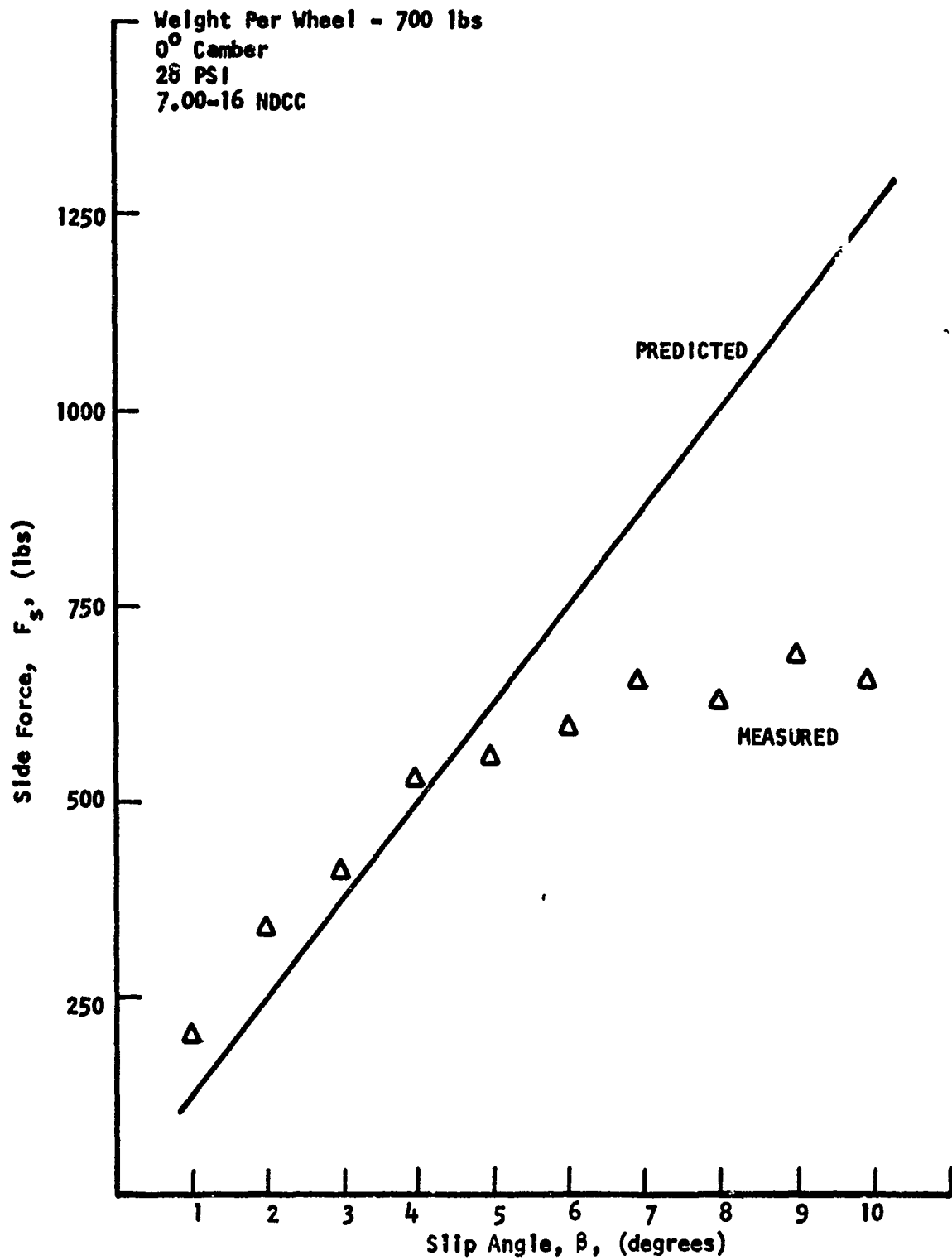SIDE THRUST VS SLIP ANGLE – 490 LBS LOAD

FIGURE 17. COMPARISON OF MEASURED AND PREDICTED
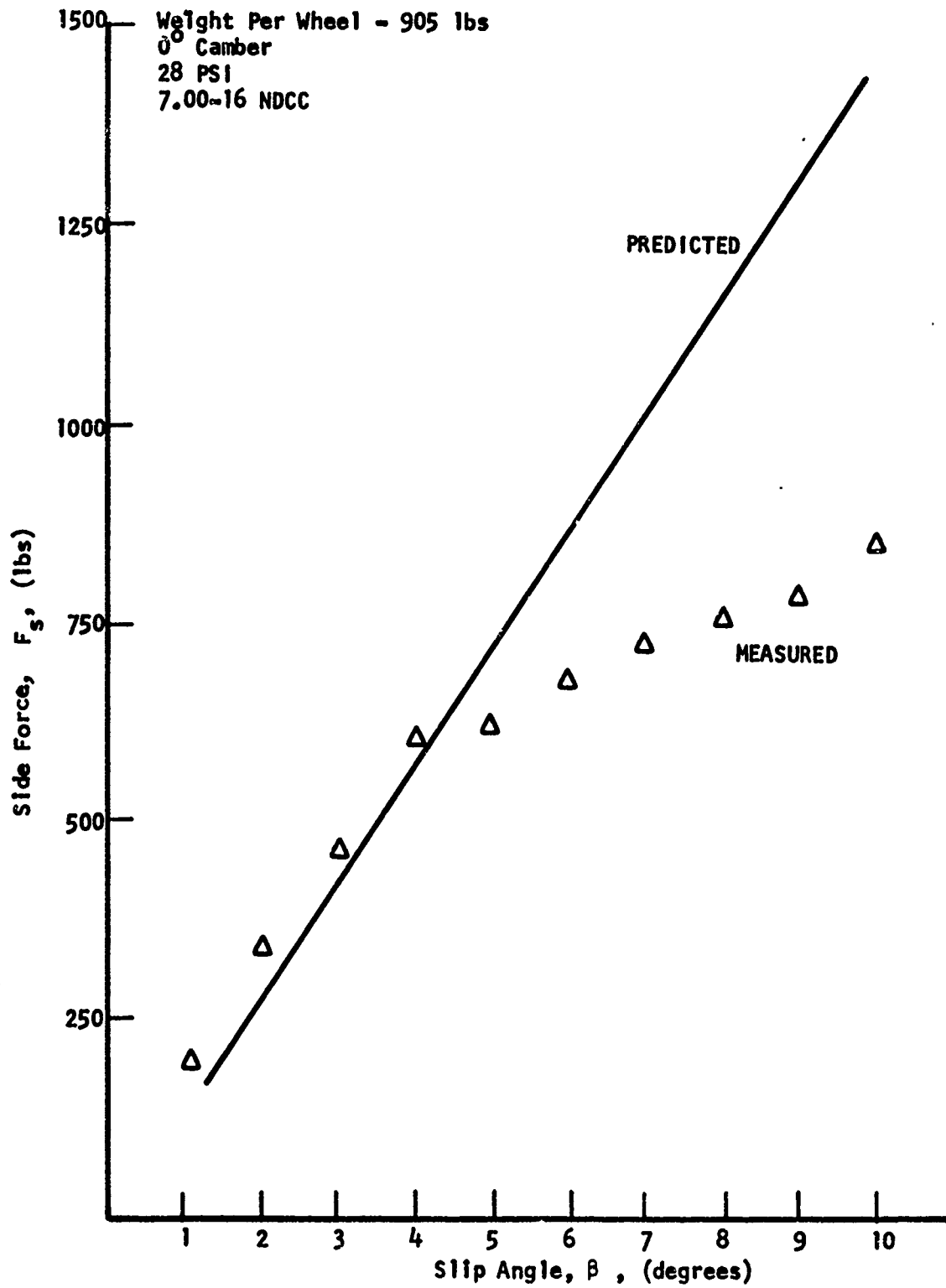SIDE THRUST VS SLIP ANGLE - 700 LB LOAD

FIGURE 18. COMPARISON OF MEASURED AND PREDICTED
SIDE THRUST VS SLIP ANGLE - 905 LBS LOAD
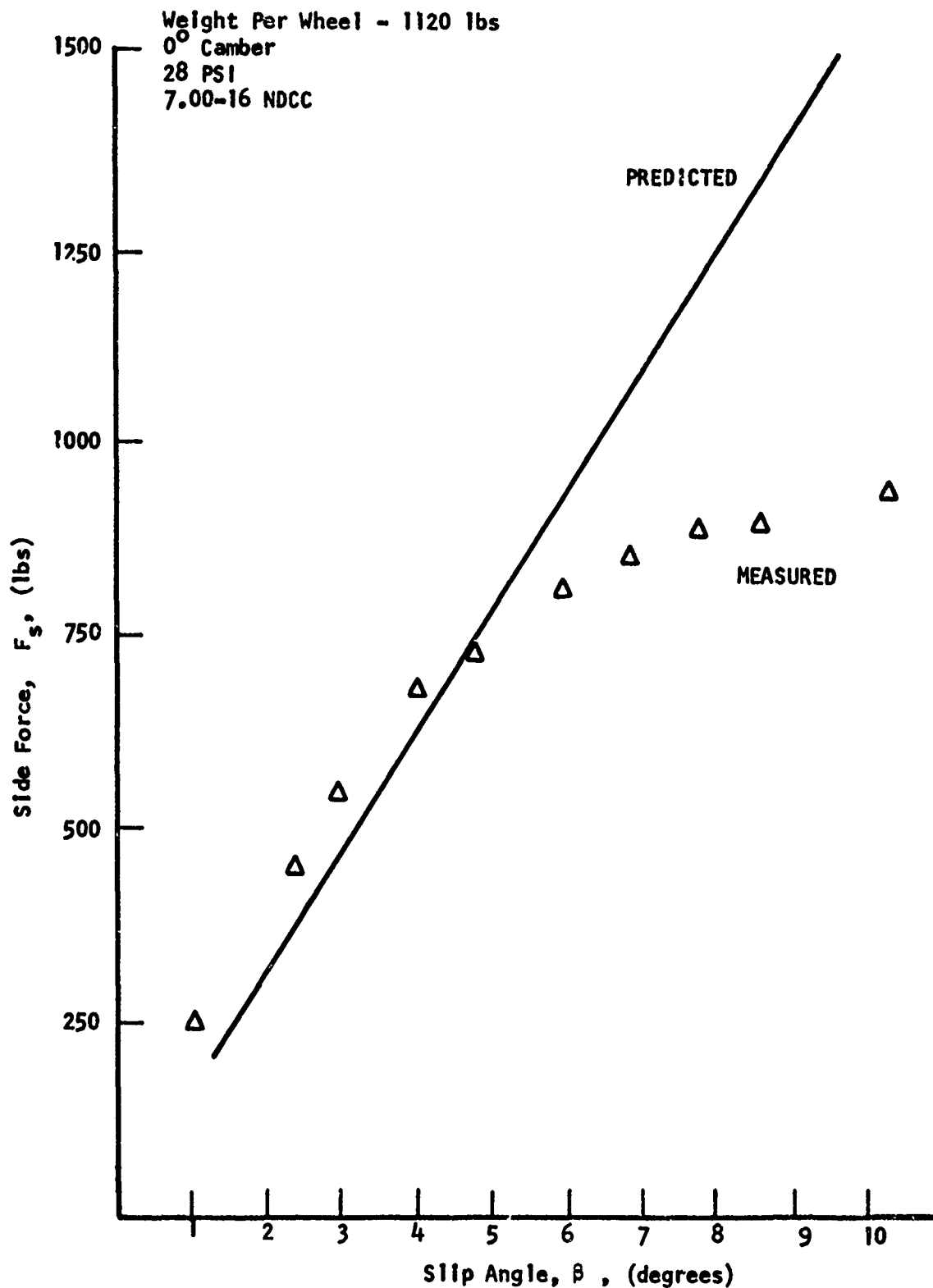
FIGURE 19. COMPARISON OF MEASURED AND PREDICTED
SIDE THRUST VS SLIP ANGLE - 1120 LBS LOAD
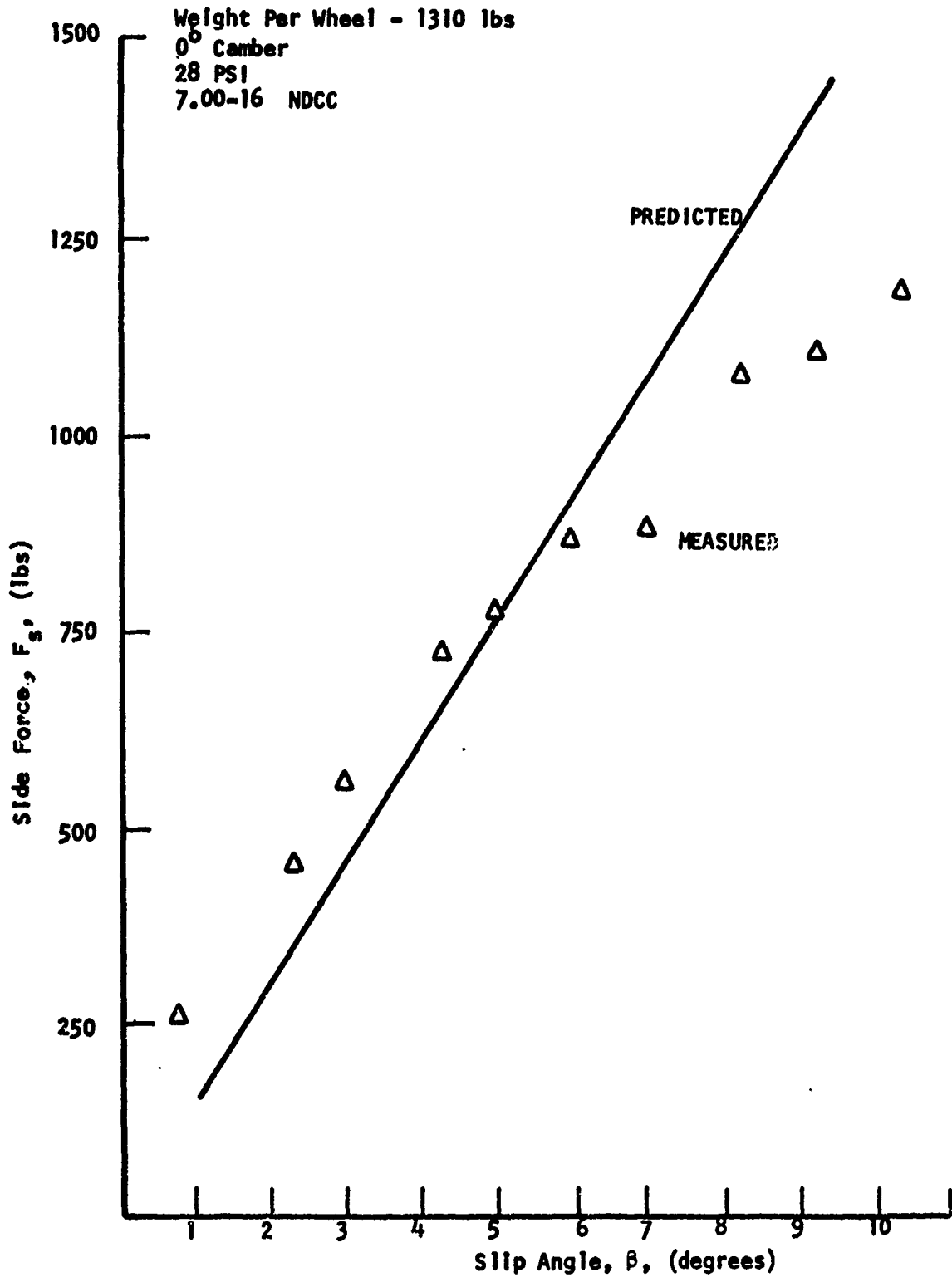
FIGURE 20.   COMPARISON OF MEASURED AND PREDICTED
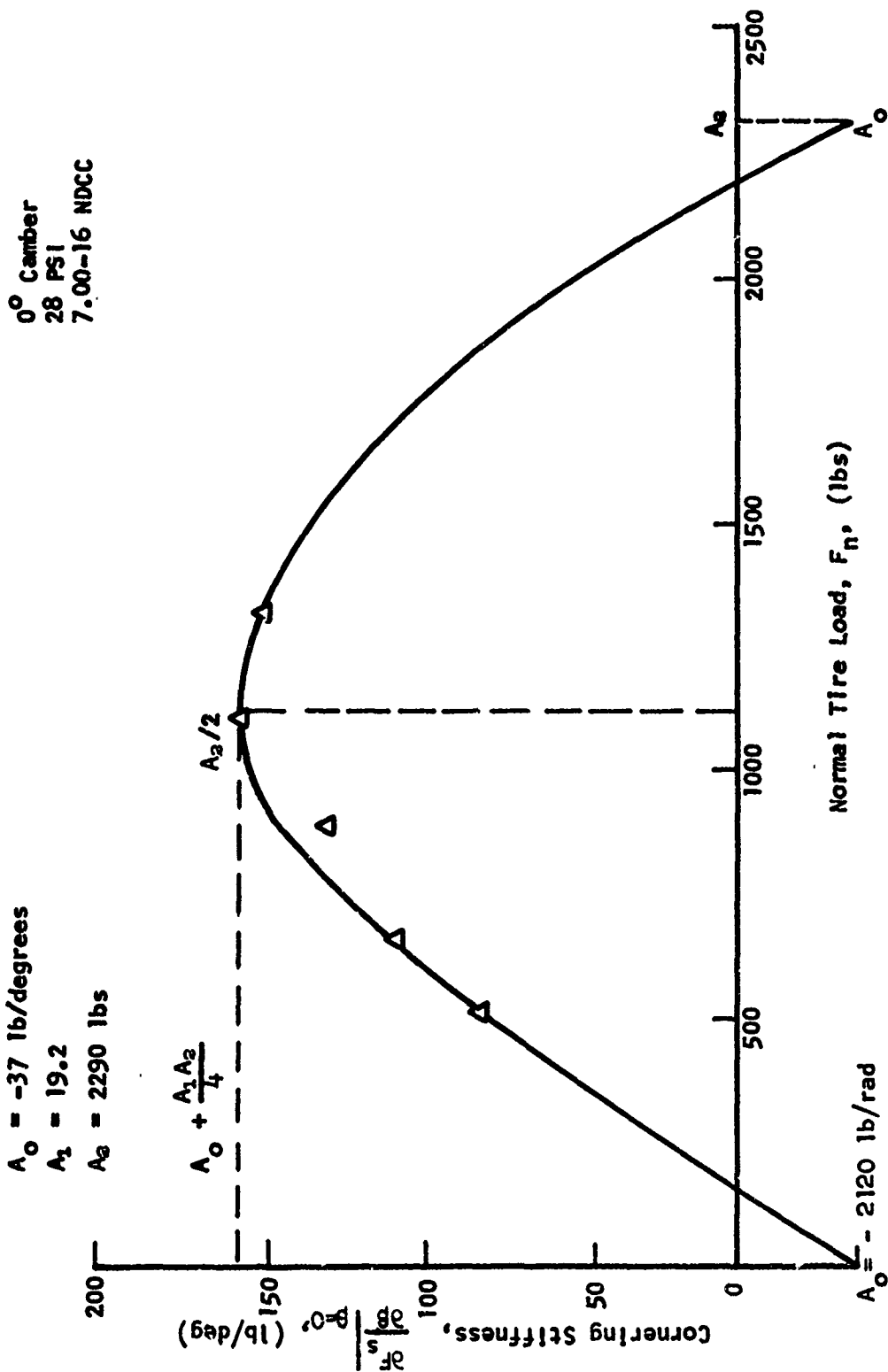   SIDE THRUST VS SLIP ANGLE - 1310 LBS LOAD

FIGURE 21. PLOT OF THE CORNERING STIFFNESS VS NORMAL LOAD FROM THE DATA OF FIGURES 24–28

$$A_o = -2120 \text{ lb/rad}$$

$$A_1 = 19.2 \tag{14}$$

$$A_2 = 2290 \text{ lb}$$

Figures 22 through 26 present the results of measured side force versus camber angle at zero slip angle for various normal loads. A listing of this data is in the appendix. These plots do not look at all like that postulated by McHenry and Deleys[5] in Figure 11 (page 21). Instead, the data appears to fall into two regimes. The initial regime extends from zero camber angle to approximately $2\frac{1}{2}^o$. In this regime the Cornering Force-Camber Angle curve is linear and has a low slope. Somewhere between 2° and 3° camber angle, depending on load, the curve makes an abrupt increase in slope.

This abrupt change of slope is a surprising result. It appears only rarely in the literature of commercial tire tests, and when it does, it occurs between 0° and $1/2^o$ camber. A possible explanation may appear in the differing geometry between military NDCC tires and commercial civilian ones. The commercial tire normally has a broad contact surface extending from sidewall to sidewall as may be seen in Figure 27. This creates a lateral force due to sidewall elasticity with the introduction of even a slightest amount of camber. However, the military tire has a rounded contact surface, and the introduction of small camber angles may not introduce much sidewall effects. Consequently, only small values of camber stiffness will be obtained at low camber angles.
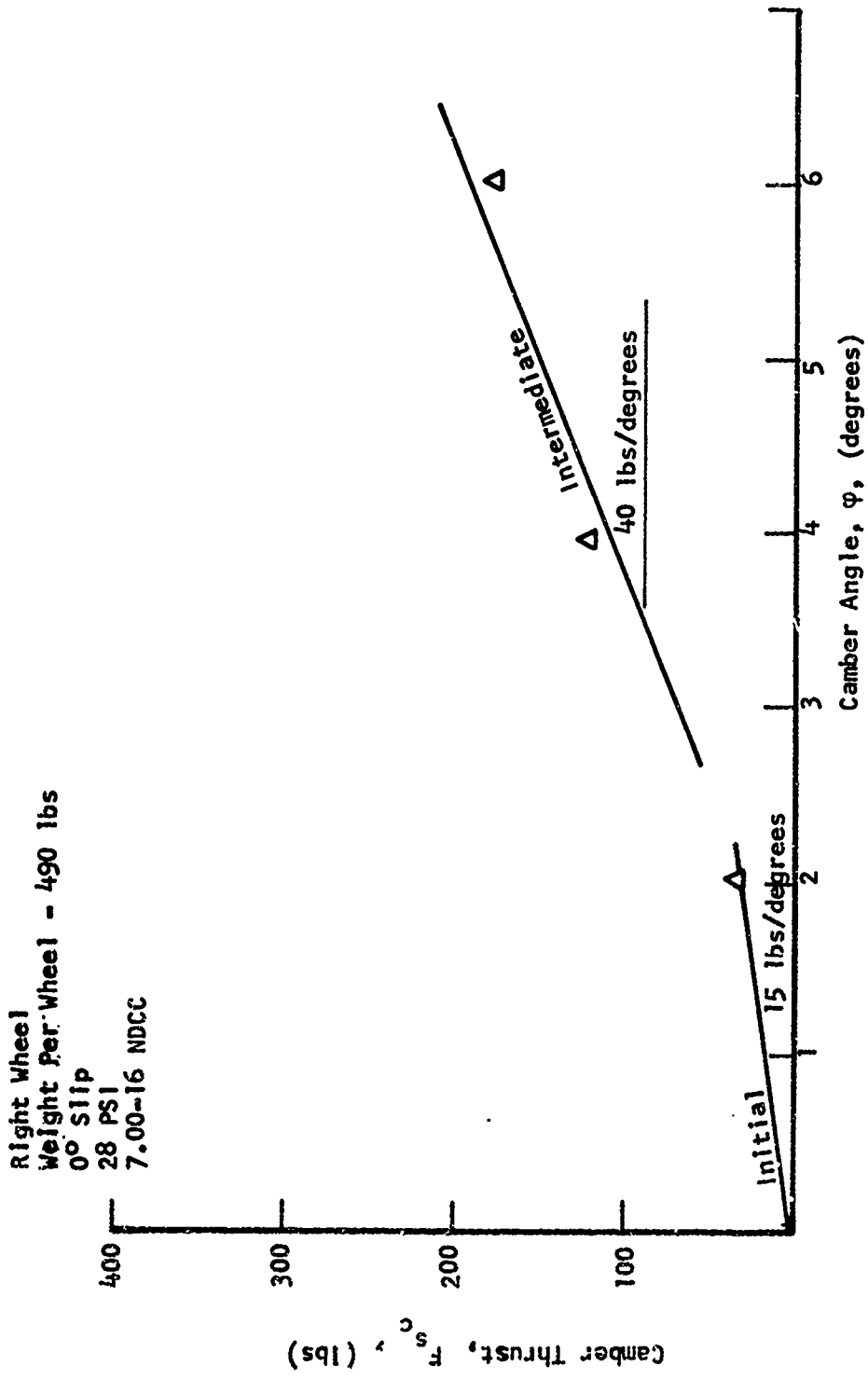
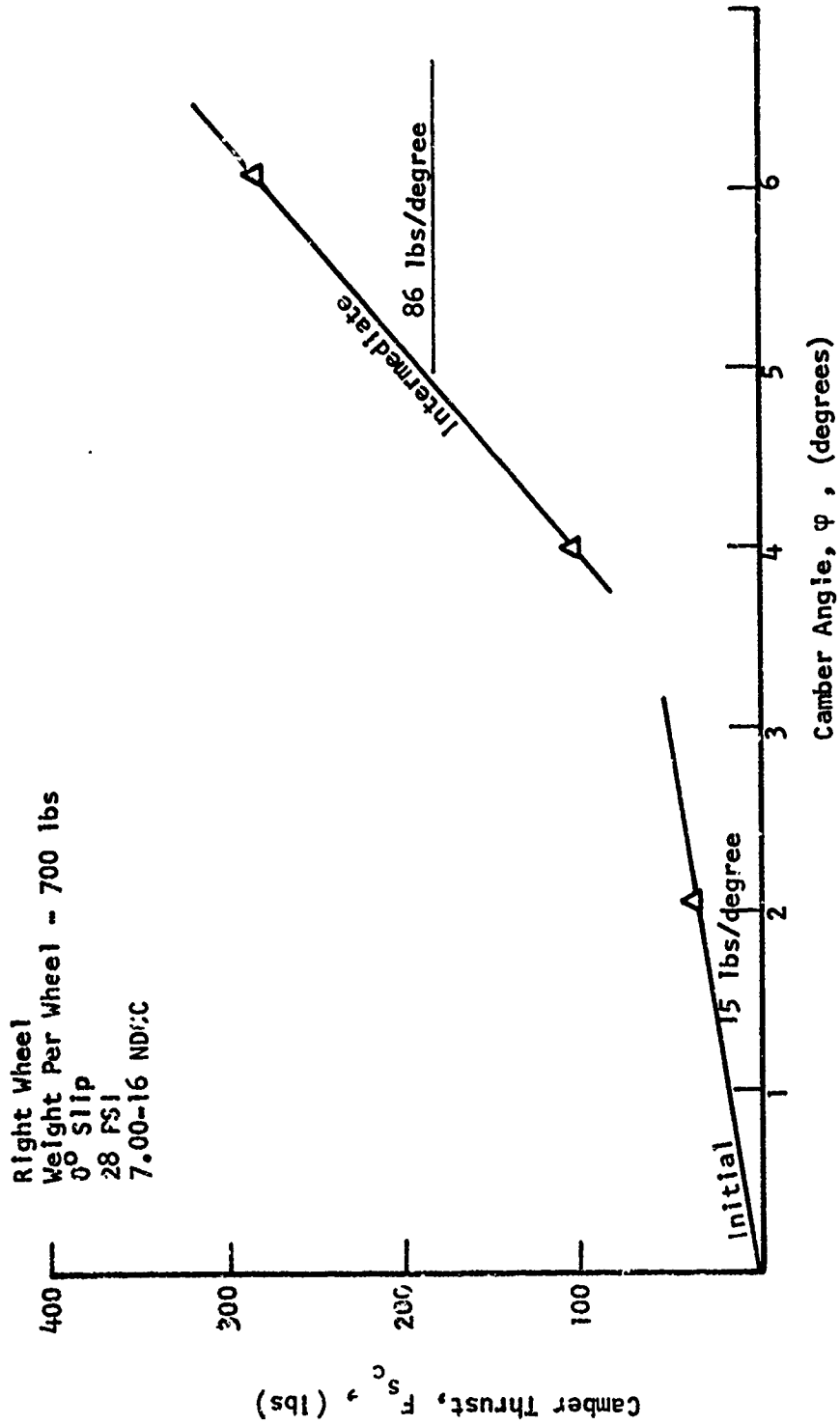FIGURE 22. CAMBER THRUST VS CAMBER ANGLE AT 490 LBS LOAD

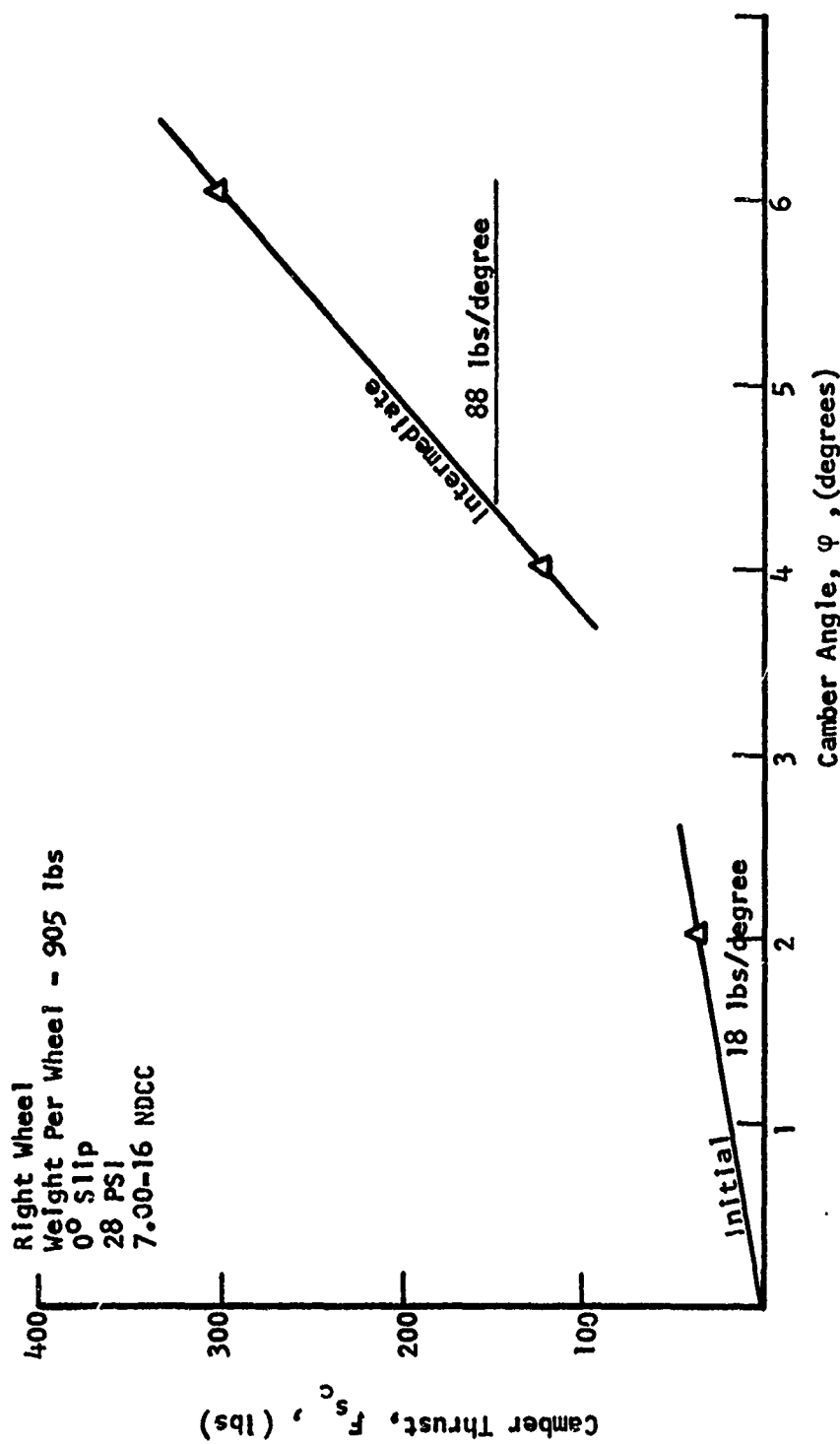FIGURE 23. CAMBER THRUST VS CAMBER ANGLE AT 700 LBS LOAD

FIGURE 24. CAMBER THRUST VS CAMBER ANGLE AT 905 LBS LOAD
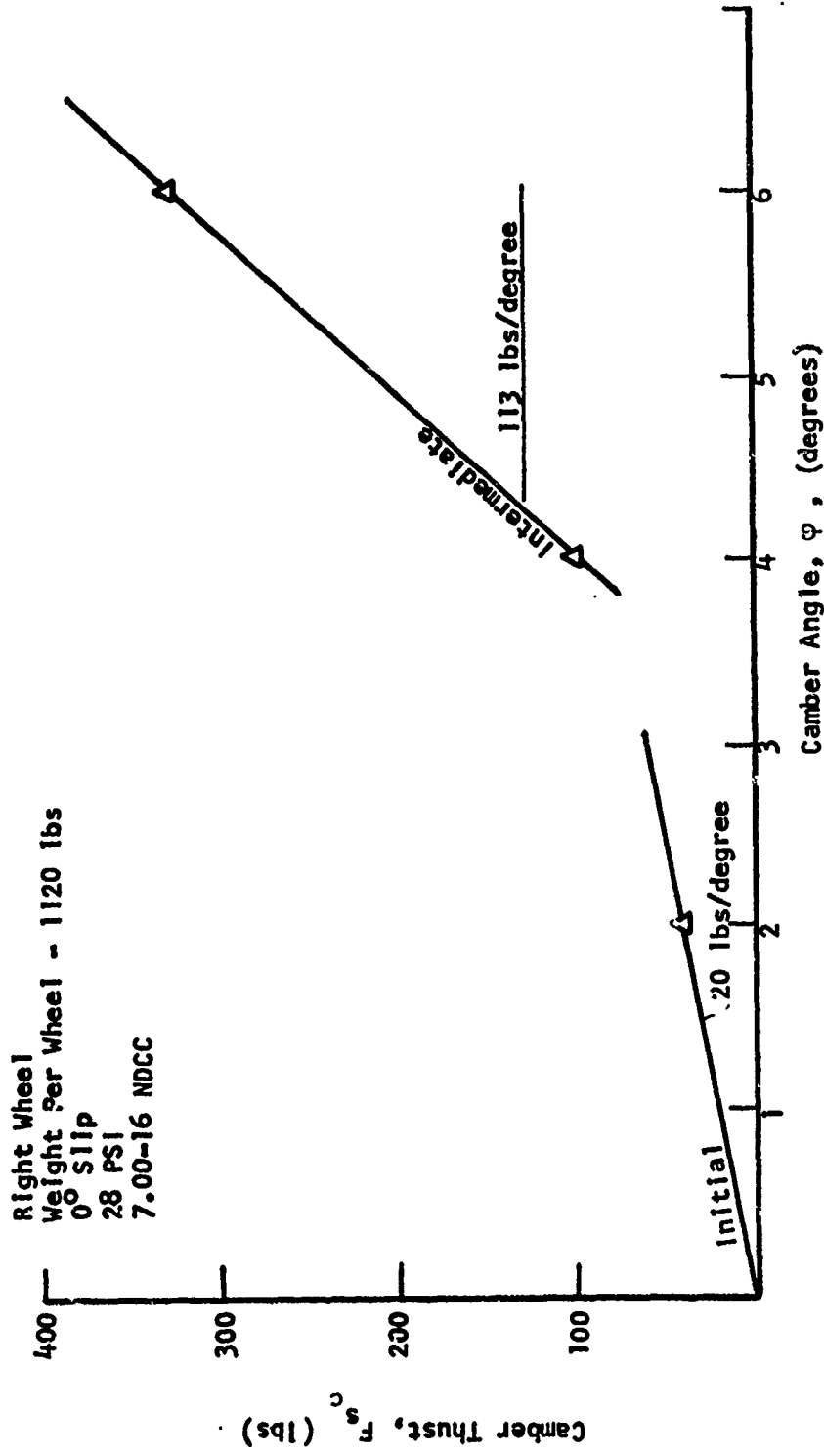
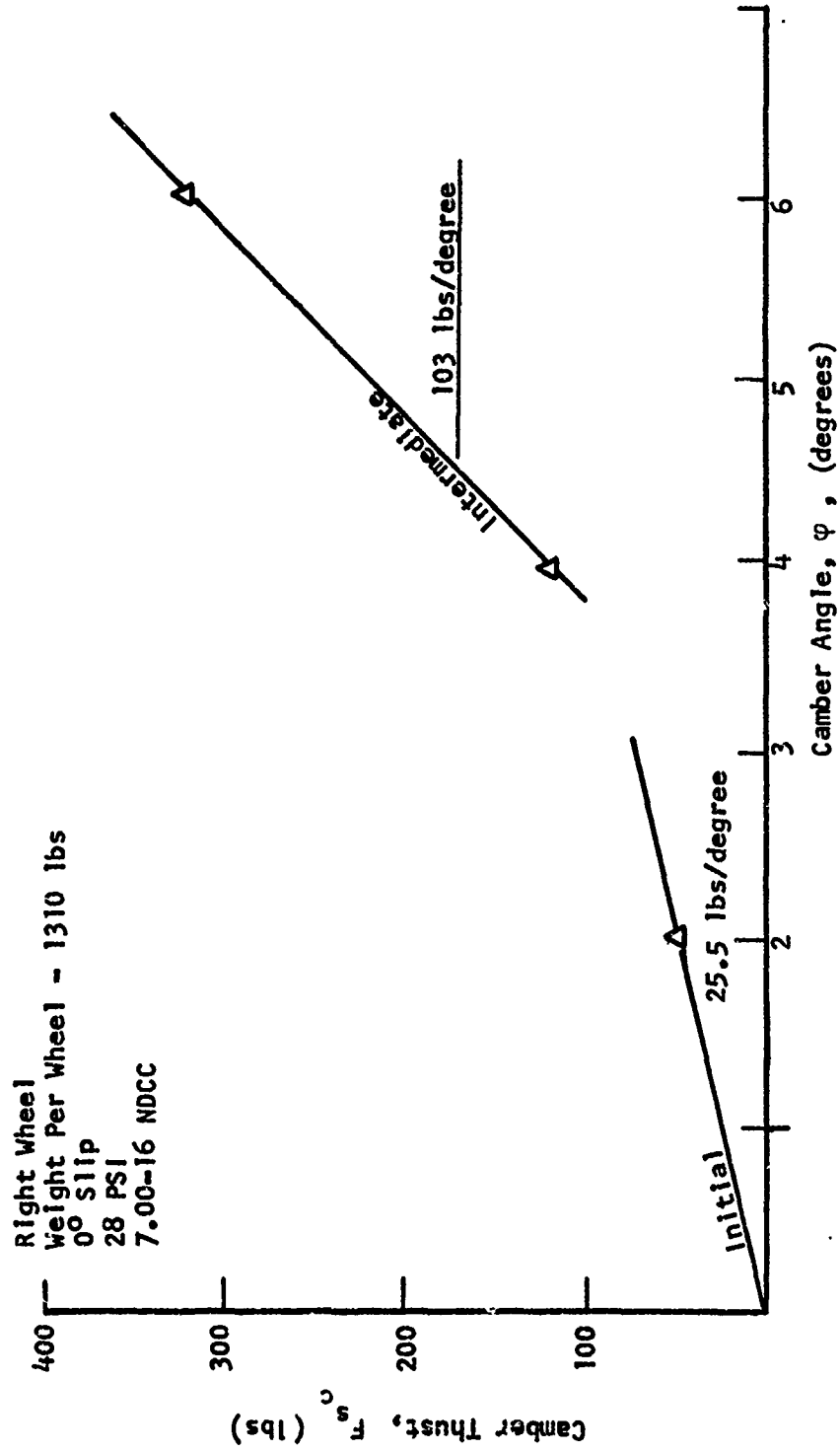FIGURE 25. CAMBER THRUST VS CAMBER ANGLE AT 1120 LBS LOAD

FIGURE 26. CAMBER THRUST VS CAMBER ANGLE AT 1310 LBS LOAD

Commercial Tire   NDCC Tire

FIGURE 27. GEOMETRIC COMPARISON OF A
COMMERCIAL TIRE AND A 7.00-16 NDCC TIRE[8]

TABLE 11

Camber Thrust Versus Normal Load

F_n (lb)	$\left.\dfrac{\partial F_s}{\partial \varphi}\right|_{\varphi=0}$ (lb/deg)
490	40
700	85
905	88
1120	113
1310	103

The slopes of the camber thrust vs camber angle are listed in Table 2 and plotted against load in Figures 28 for the initial range and in Figure 29 for the second range. The initial range slopes do not fit the parabolic relationship postulated by McHenry and Deleys, but the second range of slopes do. This is the first indication that the McHenry and Deleys relationships do not apply to military tires. When this latter data is fitted to a parabola, the other two coefficients of Equation (8) become:

$$A_3 = 11.3$$

$$A_4 = 2280 \text{ lb} \tag{15}$$

The appearance of two slopes with military tires is surprising and must be considered in the design of future vehicles. During a maneuver resulting in less than 3° of camber angle, the driver experiences an assurance of lateral stability due to minimal side thrust. When this assurance results in a maneuver increasing the camber angle beyond 3°, a sharp increase in camber thrust occurs. In conjunction
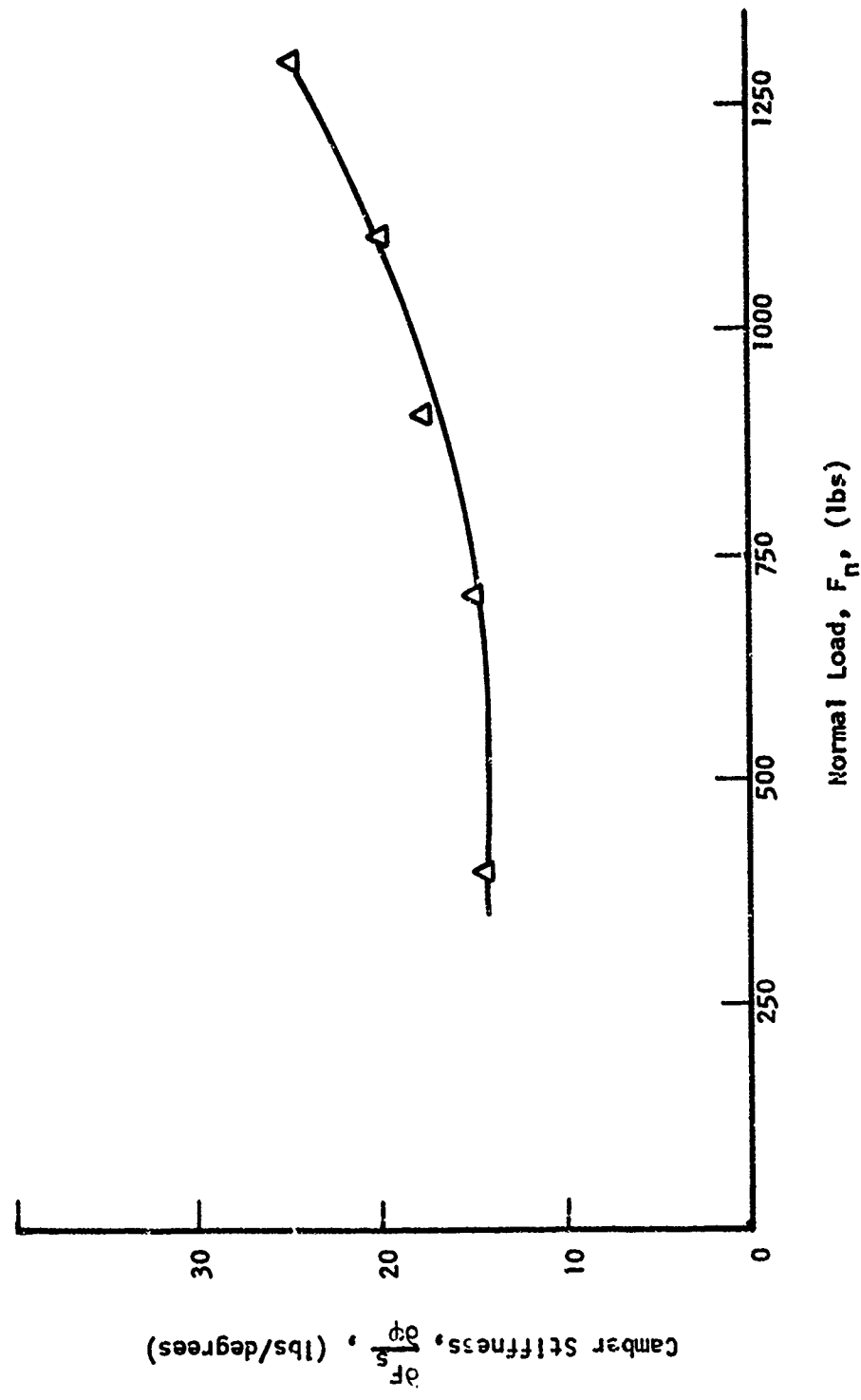
FIGURE 28. CAMBER STIFFNESS VS NORMAL LOAD – INITIAL REGIME
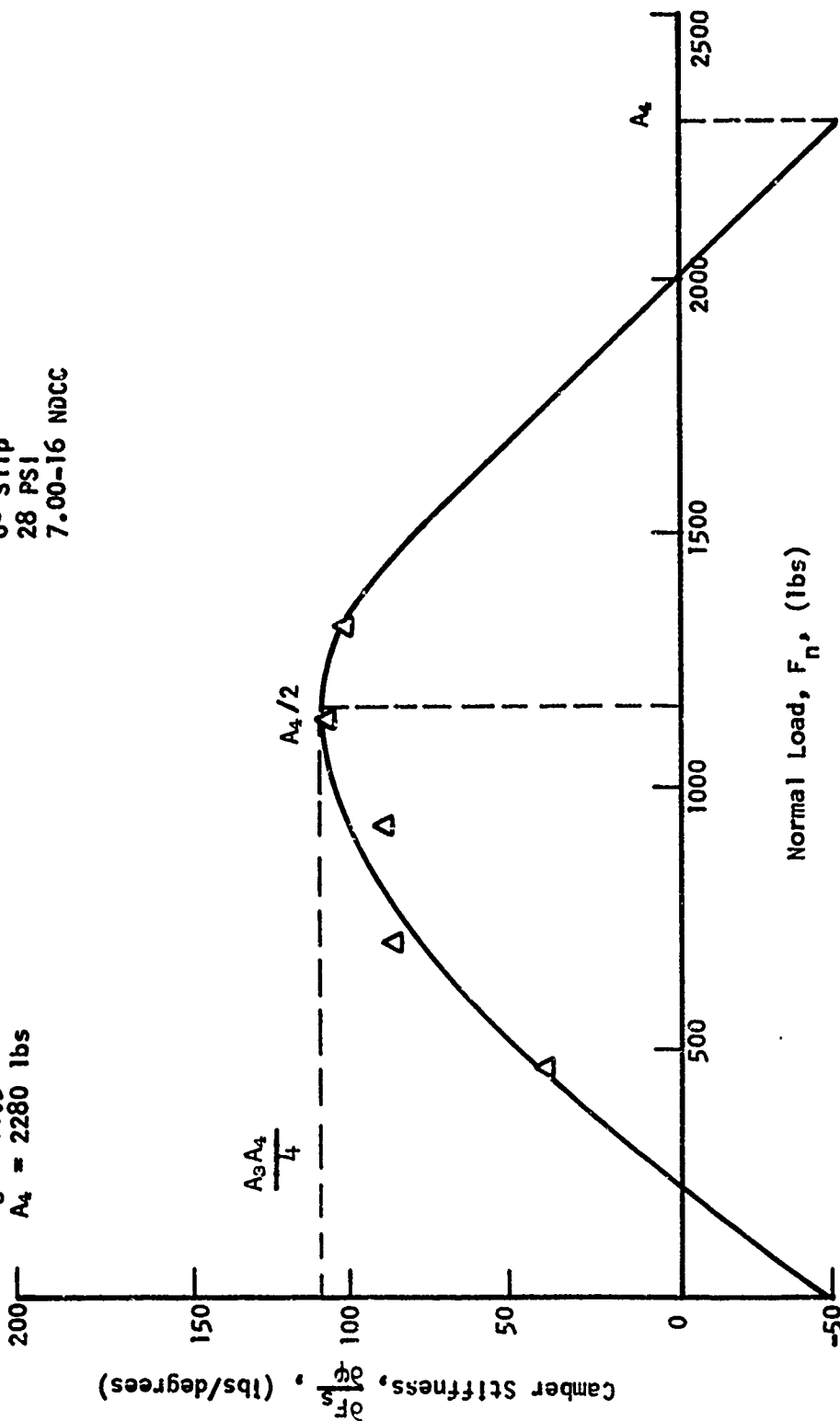
FIGURE 29. CAMBER STIFFNESS VS NORMAL LOAD – INTERMEDIATE REGIME

with other governing factors such as pavement characteristics, vehicle speed, cargo location and weight, and suspension geometry, handling qualities may abruptly change. This postulation is, at present, not yet proved, and further investigations must be conducted to verify its existence.

McHenry and Deleys analysis of side thrust prediction provided enlightening, if not conclusive, results when comparing predicted curves with measured data, as shown previously in Figures 16 through 20 and 30 through 34. (Note that these figures are corrected for trailer yaw as discussed earlier.) It must be stated that their analysis, used specifically for computer simulation of tire dynamics in vehicle-barrier impact studies, makes no pretense at predicting side force for an entire range of slip angles. Rather, it only attempts to approximate the variation of lateral force slope with normal load of 0° slip.

From Equation (13), the side thrust F_s, is a linear function of the slip angle, β, with constant normal load and 0° camber angle. From the derivation of that equation:

$$F_s = \left[\frac{A_1 F_n (F_n - A_2) - A_o A_2}{A_2} \right] \left(\frac{v}{u} - \psi' \right) \tag{16}$$

with $\beta' = 0$. Since $\beta = \left(\psi' - \frac{v}{u} \right)$,

$$F_s = \left[\frac{-A_1 F_n (F_n - A_2) + A_o A_2}{A_2} \right] \beta \tag{17}$$

Figures 16 through 20 compare the prediction of this relation to the measured values throughout the range of normal loads tested. Note that the slope of the predicted curve does not approximate the measured

slope at 0° slip, although the approximation over the range of $0 - 4^o$ is better. Figures 30 through 34 compare the predicted and measured values of side thrust for the various values of camber angle tested. The predicted curves are again linear with a constant but different slope for each F_n, as may be seen in the following equation:

$$F_s = \left[\frac{A_1 F_n (F_n - A_2) - A_o A_2}{A_2}\right] \left(\frac{v}{u} - \psi' + \beta'\right) \tag{18}$$

The measured side force data compare well only at small camber and slip angles. The predicted curves do not support these characteristics; in fact, for any normal load, the three curves relating side thrust to slip angle have a notable difference in side force as camber angle increases. Qualitatively then, the prediction theory is not supported. This may be true only of military non-directional, cross-country tires, and may be due to the roundness, stiffer sidewalls, and/or tire tread pattern. These observations lead to the conclusion that the concept of "equivalent" slip angle is not applicable to simulation of vehicle motion concerning military tires of the type tested.

It must be recognized that McHenry and Deleys derived their equations for utilization in a computer simulation involving commercial tires whose geometric and dynamic characteristics differ significantly from the military tire tested herein. The approximation of these tires may be closer, especially in the linear regime, but there is no con-sideration of saturation, where the side thrust reaches a maximum and the tire begins to slide, a phenomenon prevailing at moderate slip angles for low loads. Although, beyond the intent of this study,

Weight per Wheel, 490 lbs
28 PSI
7.00-16 NDCC

FIGURE 30. SIDE THRUST VS SLIP ANGLE FOR
VARIOUS CAMBER ANGLES AT 490 LB LOAD

FIGURE 31.   SIDE THRUST VS SLIP ANGLE FOR
VARIOUS CAMBER ANGLES AT 700 LB LOAD

FIGURE 32.   SIDE THRUST VS SLIP ANGLE FOR
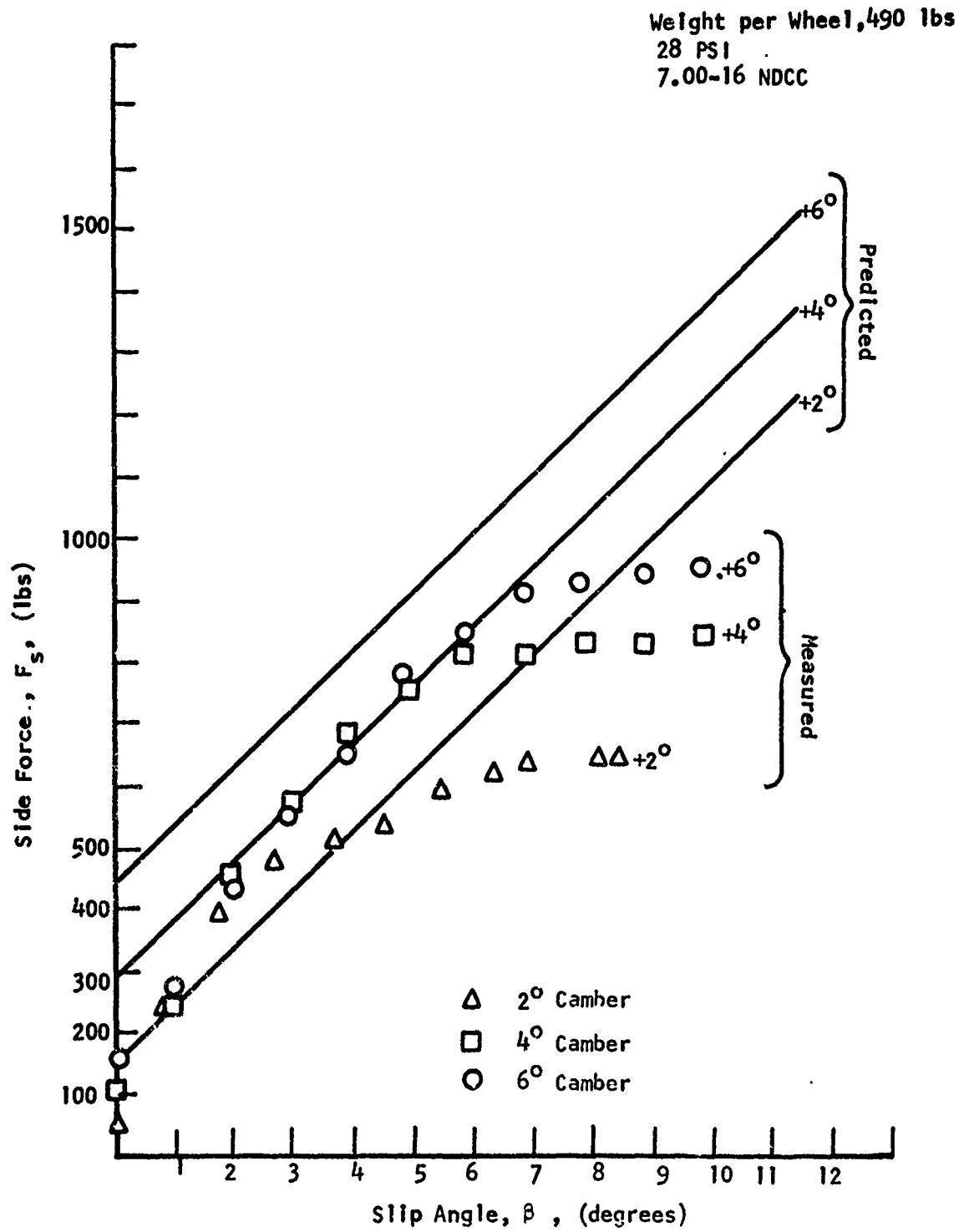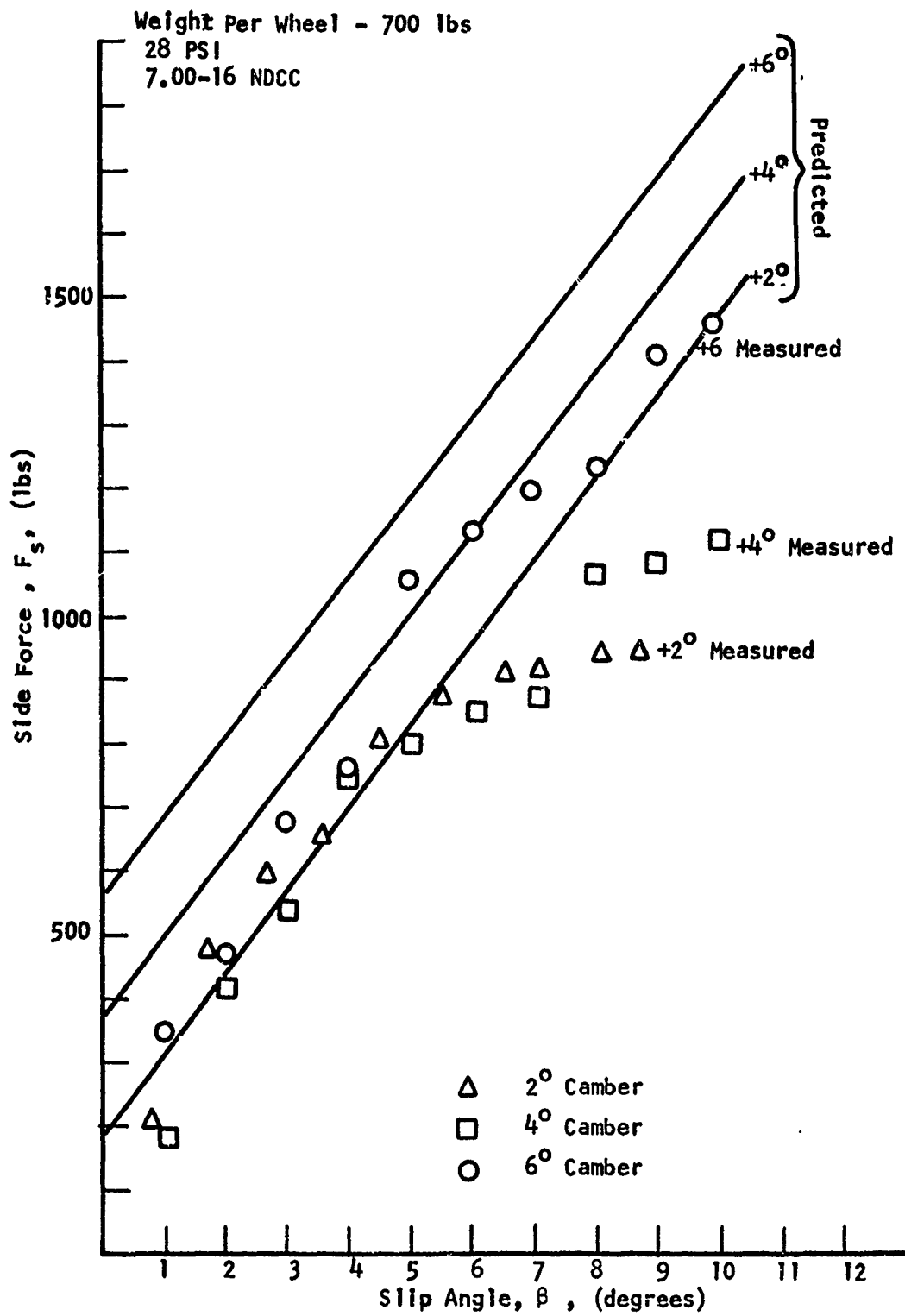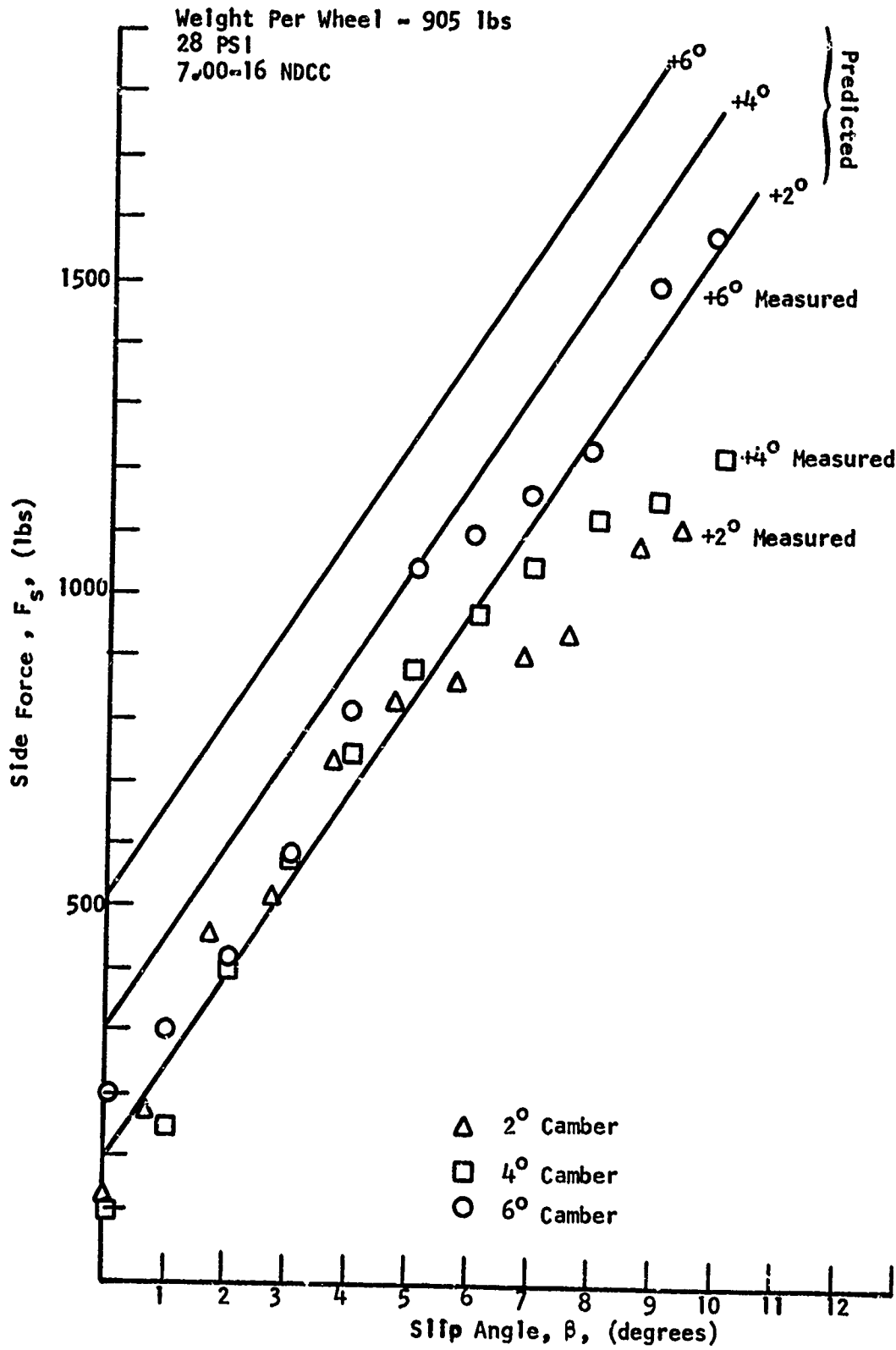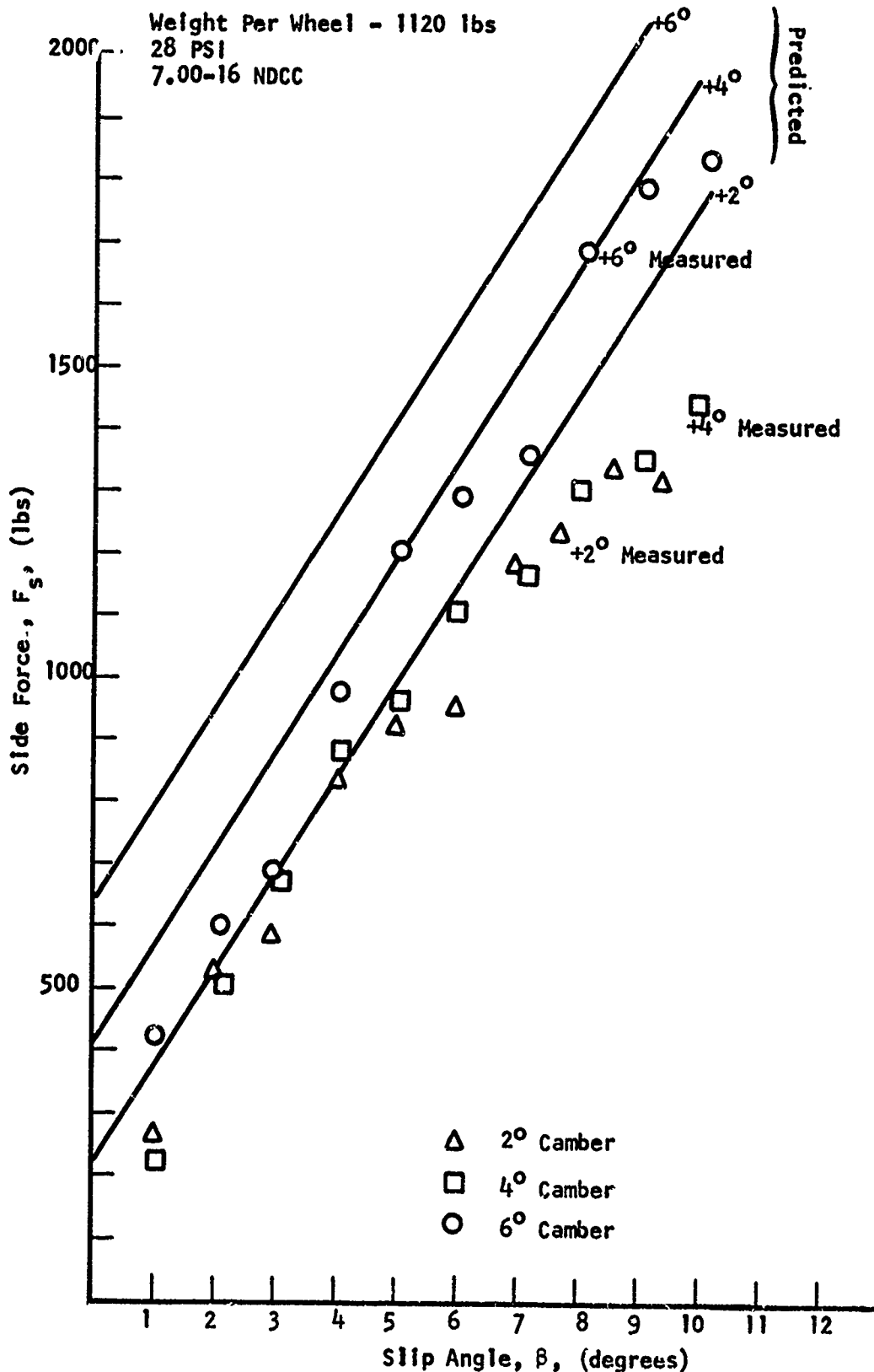VARIOUS CAMBER ANGLES AT 905 LB LOAD

FIGURE 33.   SIDE THRUST VS SLIP ANGLE FOR
VARIOUS CAMBER ANGLES AT 1120 LB LOAD
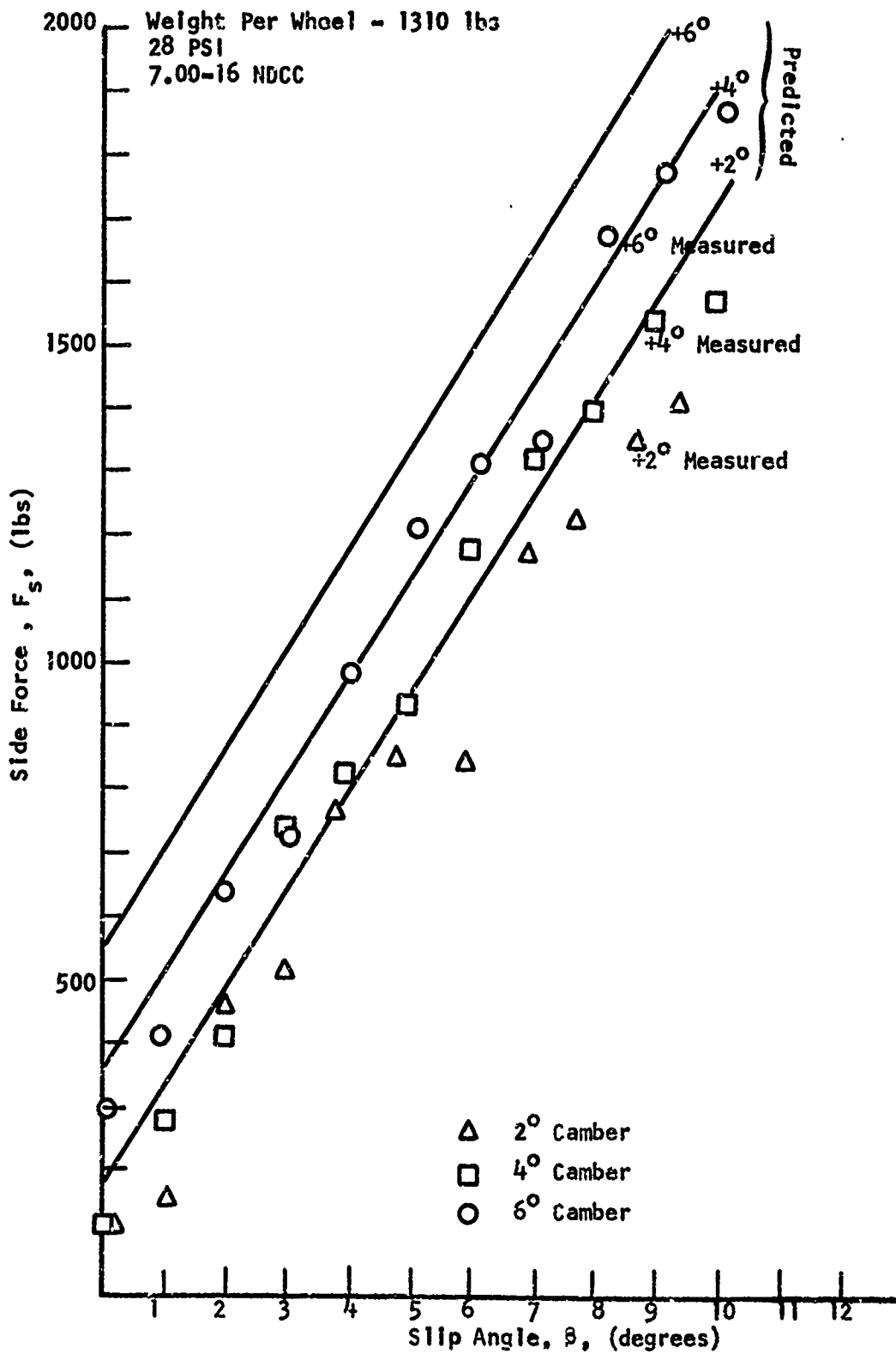
FIGURE 34.   SIDE THRUST VS SLIP ANGLE FOR
VARIOUS CAMBER ANGLES AT 1310 LB LOAD

It is possible their analysis could be altered to approximate the measured data curves by parabolic or elliptic equations more closely fitting the observed results.

CONCLUSIONS

The following conclusions are made:

(1) The generation of lateral force data along with derivation of the tire parameter coefficients for the 7.00-16 military NDCC tire provide an information base which can be correlated and integrated into the study of the handling qualities of military vehicles.

(2) McHenry and Deleys' model for camber thrust cannot be used for the prediction of the lateral force characteristics of military tires.

(3) Lateral forces in the 7.00-16 NDCC military tire in the linear region are virtually independent of camber variation for camber angles up through $+6^{\circ}$.

(4) There is an extensive initial range in the camber thrust/camber angle curve where there is but a slight increase of camber thrust with increasing camber angle. This initial range may be important in the study of military vehicle dynamics.

RECOMMENDATIONS

The following recommendations are made:

(1) A new trailer should be built or the present trailer modified to diminish internal dynamic deviations between tires resulting from inconsistent translation of forces through the wheel housing and bearings.

(2) A device should be added to the toe-in trailer to measure self-aligning torque at the tire contact patch.

(3) A program should be conducted with this tire which extends the range of loadings so that it resembles those the tire experiences in normal day-to-day use in the hands of military personnel.

(4) Extensive tests should be undertaken to determine the validity of results obtained from the toe-in trailer in relation to other types of equipment used for the measurement of tire dynamic properties.

ACKNOWLEDGEMENTS

MEASURED TIRE SIDE FORCE FOR VARIOUS CAMBER (φ) AND SLIP (β) ANGLES

7.00-16 4-PLY TIRE AT 28 PSI

NORMAL LOAD F_n, (lb)	SLIP ANGLE β, (degree)	SIDE FORCE, F_s, (lb)			
		($\varphi=0°$)	($\varphi=2°$)	($\varphi=4°$)	($\varphi=6°$)
490	-1	-	-	40	100
490	0	-	30	120	175
490	1	165	230	240	275
490	2	260	385	440	425
490	3	325	470	560	545
490	4	380	505	690	645
490	5	380	525	740	770
490	6	405	590	800	840
490	7	410	610	800	900
490	8	450	620	820	920
490	9	420	630	820	930
490	10	440	630	830	940
700	-1	-	-	50	150
700	0	-	30	125	275
700	1	200	205	250	350
700	2	340	470	500	470
700	3	410	590	675	670
700	4	530	650	850	860
700	5	540	790	975	1050
700	6	590	860	1075	1130
700	7	650	900	1150	1190
700	8	620	900	1225	1230
700	9	680	930	1250	1400
700	10	650	930	1325	1450
905	-1	-	-	-50	150
905	0	-	40	125	300
905	1	200	270	250	400
905	2	340	550	500	520
905	3	470	615	675	680
905	4	600	830	850	910
905	5	620	930	975	1140
905	6	680	960	1075	1200
905	7	720	1010	1150	1260
905	8	750	1040	1225	1330
905	9	780	1180	1250	1600
905	10	850	1205	1325	1675

(Cont'd)

MEASURED TIRE SIDE FORCE FOR VARIOUS CAMBER (φ) AND SLIP (β) ANGLES
7.00-16 NDCC TIRE AT 28 PSI

NORMAL LOAD F_n, (lb)	SLIP ANGLE β, (degree)	SIDE FORCE, F_s, (lb)			
		($\varphi=0°$)	($\varphi=2°$)	($\varphi=4°$)	($\varphi=6°$)
1120	- 1	-	-	- 50	175
1120	0	-	45	100	325
1120	1	250	270	225	425
1120	2	440	520	500	600
1120	3	540	580	675	675
1120	4	580	830	880	970
1120	5	720	920	960	1200
1120	6	800	950	1100	1280
1120	7	840	1180	1175	1350
1120	8	880	1230	1300	1675
1120	9	880	1330	1350	1775
1120	10	930	1305	1425	1825
1310	- 1	-	-	- 10	150
1310	0	-	50	120	325
1310	1	260	165	280	400
1310	2	450	460	415	625
1310	3	570	515	740	720
1310	4	720	770	820	970
1310	5	780	850	930	1190
1310	6	860	840	1165	1290
1310	7	870	1175	1315	1330
1310	8	1075	1225	1390	1650
1310	9	1100	1350	1540	1750
1310	10	1175	1400	1565	1850

REFERENCES

1. Broulhiet, G., "The Suspension of the Automobile Steering Mechanism: Shimmy and Tramp," _Bull. Soc. Ing. civ-Fr_, Vol. 78, p. 540-554, July 1925.

2. Milliken, W.F., Segal, L., Close, W. and Muzzey, C.L, Fonda, A.G., and Whitcomb, D.W., _Research in Automobile Stability and Control and in Tyre Performance_, 5 papers published by the Institute of Mechanical Engineers, on behalf of Cornell Aeronautical Laboratory, Inc., 1956.

3. Segel, L., "Theoretical Prediction and Experimental Substantiation of the Response of the Automobile to Steering Control," in Milliken, et al, above.

4. Fiala, E., "Lateral Forces on Rolling Pneumatic Tires," _Zeitschrift V.D.I._, Vol. 96, No. 29, October 1954.

5. McHenry, Raymond R. and Deleys, Norman, J., "Vehicle Dynamics in Single Vehicle Accidents Validation and Extensions of a Computer Simulation," Cornell Aeronautical Laboratory, Inc., Technical Report No. PB182663, Buffalo, New York, December 1968.

6. Jurkat, M. P., "A Theoretical Investigation of the Stability of the M-151, 1/4-Ton Military Truck", DL Report 1420, September 1969.

7. _Automotive Engineering_, United States Military Academy, West Point, New York, Department of Ordnance, Vol. II, 1969.

Refererces (continued)

8. Milliken, W. F., Whitcomb, D. W., Segel, L., et al, "Research in Automobile Stability and Control and in Tire Performance", Automobile Division, Institute of Mechanical Engineers, 1956.

9. Nothstine, J. R. and Beauvais, F. N., "Laboratory Determination of Tire Forces", Society of Automotive Engineers International Meeting, Montreal, Canada (date unknown).

10. Kamm, I. O. and Starrett, J. A., "Lateral and Longitudinal Force Measurement on Representative Automobile Tires", Davidson Laboratory, Stevens Institute of Technology, Technical Report 1363, January 1969.

BIBLIOGRAPHY

1. Clark, Samuel K., "The Rolling Tire Under Load," Society of Automotive Engineers, Mid-year Meeting, Chicago, Illinois, May 17-21, 1965.

2. Dodge, Richard N., "The Dynamics Stiffness of a Pneumatic Tire Model," SAE, Mid-year Meeting, Chicago, Illinois, May 17-21, 1965.

3. Ellis, J. R., Vehicle Dynamics, London Business Books Limited, London, England, 1969.

4. Frank, F., "Kautschuk Gummi," 18, 515, 1965.

5. Frank, F. and Hofferberth, W., "Mechanics of the Pneumatic Tire," Deutsche Dunlop Gummi Compagnie AG, Nanau, Germany, 1965. (Translation by G. Leuca)

6. Jurkat, M. P., "A Theoretical Investigation of the Stability of the M-151, 1/4-Ton Military Truck," Davidson Laboratory, S.I.T., Report 1420, September 1969.

7. Heitzman, E. J., "A Tire Performance Rating System for Vehicle Safety," Automobil ⎿ velopment Associates, Technical Report No. 4-1, Princeton, New Jersey, March 1966.

8. Leviticus, L. I., "Evaluation of NDCC and Mud and Snow Tires in Soft Soil," Davidson Laboratory, S.I.T , Report 1502, January 1971.

9. Neilson, I. S., "An Introductory Discussion of the Factors Affecting Car Handling," Road Research Laboratory, Crowthorne, England, 1968.

Bibliography (continued)

10. Owen, R. E. and Ladd, M. R., "Accudrive Stability with Comfort,"
    SAE Paper 690490, May 1969.

11. Rice, R. S.,Jr., and Milliken, W. F.,Jr., "The Effect of Loadings
    and Tire Characteristics on the Steering Behavior of an Automobile,"
    Cornell Aeronautical Laboratory, Inc., 1968.

12. Segel, Leonard, "Theoretical Prediction and Experimental Sub-
    stantiation of the Response of the Automobile to Steering Control,"
    Cornell Aeronautical Laboratory, Inc., Buffalo, New York, August
    1956.

13. Stocker, A. J., "Tractional Characteristics of Automobile Tires,"
    Texas A&M University, College Station, Texas, November 1968.

14. Strumpf, Albert, "Notes on Automobile Stability," Davidson
    Laboratory, S.I.T., Technical Note 391, April 1965.

15. Tiffany, N. O., Cornell, G. A., and Code, R. L., "A Hybrid Simula-
    tion of Vehicle Dynamics and Subsystems," Bendix Research Labora-
    tories, SAE Paper, Automotive Engineering Congress, Detroit,
    Michigan, January 12-16, 1970.

16. "Tyre Construction Advances Significant to the Engineer,"
    Automotive Design Engineering, April, 1968.

17. Wakefield, Ronald, "Suspension and Handling," Road and Track,
    June 1970.